

## 12-5.1 Coupled Array Pattern Calculation

Section 12-5 describes array pattern computation composed of coupled V-dipoles elements. The levels of the standing wave sinusoidal currents determine the patterns of arrays of V-dipoles which leads to a coupled impedance matrix model of the array.  $[V] = [Z][I]$  where  $[V]$  is the feeding voltage vector,  $[Z]$  is the impedance matrix, and  $[I]$  the vector of dipole input currents. We calculate the mutual impedance matrix term by term from the coupling between two dipoles depending on their positions and orientation. We compute feed currents from  $[I] = [Z]^{-1}[V]$

The supplied program **XADEF** generates an array geometry and excitation file. For example, generate an array for use in scan element pattern for elements in a 19-element hex array where the center element fed and the surrounding elements are only loaded. The elements are spaced  $0.6\lambda$  at 1 GHz. Start with all elements fed at -100 dB and then edit the amplitude of the first element (center): **ed,am,1**

```
C:\Phased_Array>xadef
Enter input 0 keyboard, 1 file 0
Enter File Name vds19.arr
Enter units: 1 in., 2 ft, 3 cm, 4 m 1
New File? y
Enter Frequency (GHz) 1
xadef: ad,he,19
Enter Ampl (dB), Phase -100,0
Enter Rotation of Hex 0
Enter Element Spacing in. 7.082
move: ex
Enter Final New Z axis Rotation of Antennas (array) 0
xadef: ed,am,1
Element No: 1
Location: X = 0.000 Y = 0.000 Z = 0.000
Ampl(dB) = -100.00 Phase = 0.00
Euler Angles = 0.00 0.00 0.00
Enter New Amplitude (dB) 0
xadef: li,fi

File:vds19.arr
```

No	X	Location Y	Z	Ampl(dB)	Element Phase	Euler Angles		
1	0.000	0.000	0.000	0.00	0.00	0.00	0.00	0.00
2	7.082	0.000	0.000	-100.00	0.00	0.00	0.00	0.00
3	3.541	6.133	0.000	-100.00	0.00	0.00	0.00	0.00
4	-3.541	6.133	0.000	-100.00	0.00	0.00	0.00	0.00
5	-7.082	0.000	0.000	-100.00	0.00	0.00	0.00	0.00
6	-3.541	-6.133	0.000	-100.00	0.00	0.00	0.00	0.00
7	3.541	-6.133	0.000	-100.00	0.00	0.00	0.00	0.00
8	14.164	0.000	0.000	-100.00	0.00	0.00	0.00	0.00
9	10.623	6.133	0.000	-100.00	0.00	0.00	0.00	0.00
10	7.082	12.266	0.000	-100.00	0.00	0.00	0.00	0.00
11	0.000	12.266	0.000	-100.00	0.00	0.00	0.00	0.00
12	-7.082	12.266	0.000	-100.00	0.00	0.00	0.00	0.00
13	-10.623	6.133	0.000	-100.00	0.00	0.00	0.00	0.00
14	-14.164	0.000	0.000	-100.00	0.00	0.00	0.00	0.00
15	-10.623	-6.133	0.000	-100.00	0.00	0.00	0.00	0.00
16	-7.082	-12.266	0.000	-100.00	0.00	0.00	0.00	0.00
17	0.000	-12.266	0.000	-100.00	0.00	0.00	0.00	0.00
18	7.082	-12.266	0.000	-100.00	0.00	0.00	0.00	0.00
19	10.623	-6.133	0.000	-100.00	0.00	0.00	0.00	0.00

```
xadef: _
```

## Chapter 12 Phased Arrays

A list of commands to **XADEF** are listed by typing: **??**.

**xadef: ??**

### Directive Array File Definition Directives

1. **<??.<pr>>**. . . . List Directives
2. **<ad,el,<#>**. . . . Add, Elements,<Number>
3. **<ad,re,<#>,<ar>>** . Add, Rectangular Array
4. **<ad,he,<#>,<ar>>** . Add, Hexangular Array
5. **<ad,ci,<#>,<ar>>** . Add, Circular Array
6. **<ad,ep,<#>,<ar>>** . Add, Elliptical Array
7. **<ad,ar,<#>,<ar>>** . Add, Arc Array
8. **<ad,ca,<#>,<ar>>** . Add, Cap Array
9. **<ad,co,<#>,<ar>>** . Add, Cone Array
10. **<ad,tr,<#>,<ar>>** . Add, Triangular Spaced Array
11. **<ad,ri,<#>,<ar>>** . Add, Ring filled Array
12. **<ad,sp,<#>,<ar>>** . Add, Spherical Array
12. **<ad,ic,<#>,<ar>>** . Add, Icosahedron Spherical Array
13. **<li,fi,<pr>>** . . . List File
14. **<li,<NUMBER>>**. . . List Element <NUMBER>
15. **<ed,lo,<#>**. . . . Edit Location <NUMBER>
16. **<ed,am,<#>**. . . . Edit Amplitude <NUMBER>
17. **<ed,am,gr,<#>,<#>** . Edit Amplitude Group,<#>,to<#>
18. **<ed,ph,<#>**. . . . Edit Phase <NUMBER>
19. **<ed,eu,<#>**. . . . Edit Euler Angles <NUMBER>
20. **<ch,fr>**. . . . . Change Frequency
21. **<ex>** . . . . . Exit xadef

**xadef:**

See Section 4-27 for more detail instructions for **XADEF**.

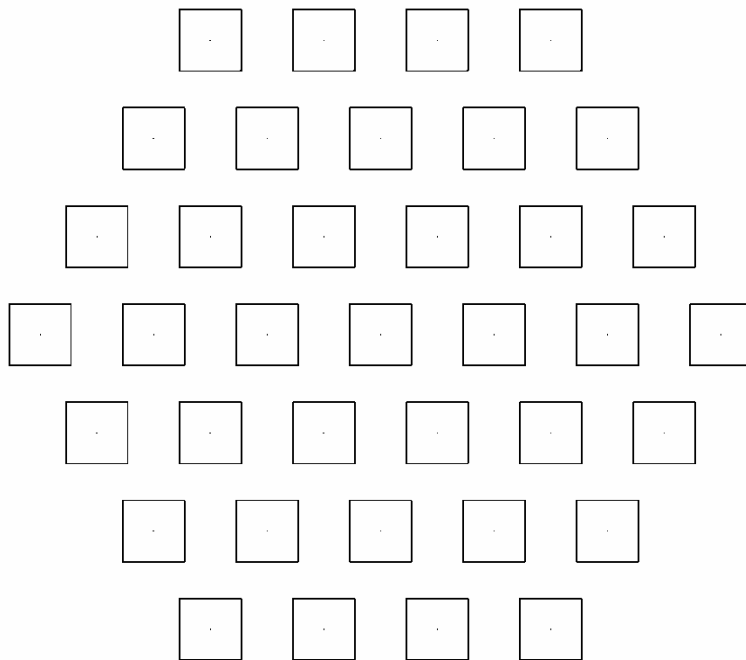


**Figure 12-5.1.1** Hexagonal Array of 37 elements spaced  $0.6\lambda$ ; Center #1 X-axis: #2, #8, #20

## Chapter 12 Phased Arrays

### elements

**VDAIMC** computes characteristics of an array of V-dipoles mounted on an infinite ground plane.

```
C:\Phased_Array>vdaimc
Enter input: 0 keyboard, 1 file 0
Enter units: 1 in, 2 cm, 3 ft, 4 m 1
Enter array efficiency: 0 none, 1 uniform, 2 Tapered Distr. 0
```

The program can be run by using keyboard inputs or an input text file. Equation (3-30) can be applied to compute array element efficiency by using the mutual impedance elements when all elements are fed. In this case only the center element is fed, so array efficiency is not selected. Selecting 1 computes a uniformly fed array ignoring the amplitudes in the XADEF array file, while selecting 2 uses the amplitude distribution. See Section 4-28 for a more thorough discussion and examples. By combining Equation (3-30) with Equation (12-17) directivity is eliminated and we are left with antenna element efficiency.

$$Efficiency = \frac{\sum_{i=1}^N |E_i|^2}{\sum_{i=1}^N \sum_{j=1}^N \begin{bmatrix} R_{ij} \\ R_{11} \end{bmatrix} Re \begin{bmatrix} E_j \\ E_i \end{bmatrix} |E_i|^2}$$

```
Enter 1 to use previous matrix and inverse 0
Enter Name of XADEF File vds19.arr
Change of distribution only? n
Enter Length of dipole 5.31
Enter Radius of dipole .07
Enter element tilt from horizontal 30
Enter Height of dipole over ground plane 3.54
Enter points in self, mutual impedance integrals 201,21
Enter normalized frequency 1
Write adjusted XADEF file with mutual coupling? y
Enter scan direction Theta, Phi 0,0
Enter new file name for array coefficients vds19n.arr
```

**VDAIMC** stores the mutual coupling matrix and its LU decomposition to reduce runtime for subsequent runs. The matrix is independent of amplitude and phase distribution when using other XADEF array files or scan phasing. The physical optics gain biased current of a single V-dipole are also stored to be recall, as well.

The program calls for input of the V-dipole dimensions. Two filamentary dipoles are spaced the rod radius with many points in the integral (201 in this case) for the self-impedance by using mutual impedance. Pattern calculation requires fewer points (21) along each pole. **XADEF** has a frequency associated with the array file. This frequency can be shifted by the frequency normalization factor; in this case frequency = 1 GHz.

**VDAIMC** will write an output XADEF array file with amplitude and phase adjusted for mutual coupling by using the inverse impedance matrix and initial feeding distribution so it can be inspected and with a record of element positions. The file amplitudes are adjusted to normalized (1 W) amplitudes.

## Chapter 12 Phased Arrays

XADEF file: vds19n.arr

Length units: in.

File:vds19n.arr

No	Location			Element		Euler Angles		
	X	Y	Z	Ampl(dB)	Phase			
1	0.000	0.000	0.000	-0.49	-2.18	0.00	0.00	0.00
2	7.082	0.000	0.000	-18.03	147.63	0.00	0.00	0.00
3	3.541	6.133	0.000	-18.69	89.89	0.00	0.00	0.00
4	-3.541	6.133	0.000	-18.69	89.89	0.00	0.00	0.00
5	-7.082	0.000	0.000	-18.03	147.63	0.00	0.00	0.00
6	-3.541	-6.133	0.000	-18.69	89.89	0.00	0.00	0.00
7	3.541	-6.133	0.000	-18.69	89.89	0.00	0.00	0.00
8	14.164	0.000	0.000	-32.42	-23.11	0.00	0.00	0.00
9	10.623	6.133	0.000	-25.45	-66.72	0.00	0.00	0.00
10	7.082	12.266	0.000	-30.32	-135.25	0.00	0.00	0.00
11	0.000	12.266	0.000	-25.58	-77.26	0.00	0.00	0.00
12	-7.082	12.266	0.000	-30.32	-135.25	0.00	0.00	0.00
13	-10.623	6.133	0.000	-25.45	-66.72	0.00	0.00	0.00
14	-14.164	0.000	0.000	-32.42	-23.11	0.00	0.00	0.00
15	-10.623	-6.133	0.000	-25.45	-66.72	0.00	0.00	0.00
16	-7.082	-12.266	0.000	-30.32	-135.25	0.00	0.00	0.00
17	0.000	-12.266	0.000	-25.58	-77.26	0.00	0.00	0.00
18	7.082	-12.266	0.000	-30.32	-135.25	0.00	0.00	0.00
19	10.623	-6.133	0.000	-25.45	-66.72	0.00	0.00	0.00

The coupling between element 1 (center) and next element along the  $x$ -axis (#2) is  $18.03 - 0.49 = 17.54$  dB; greater than the 20 dB two element  $E$ -plane coupling shown in Figure 6-10.1.10 due to composite coupling of all elements, etc.

```
Use new array coefficients? n
Enter matrix file vds19m.dat
Enter element current file vds19m.cur
Enter scan direction Theta, Phi 0,0
Include mutual coupling effects? y
Pattern? y
```

We have a choice of using the new array coefficients in following pattern calculations, but we should not answer 'Yes' to the include mutual coupling effects 4 lines later because mutual coupling effects will be applied twice.

The next line asks for the storage file name of the mutual impedance and its LU decomposition (stored together). This followed by single V-dipole currents file. If we use these on following runs,

## Chapter 12 Phased Arrays

```
Pattern? y
Enter Output Code:
  1 E Theta, 2 E Phi 3 RHC, 4 LHC, 5 Max. Lin., 6 Min. Lin.,
  7 +45 Comp., 8 -45 Comp., 9 Power 1
Enter type (1) Conical, (2) Great Circle,
3 Theta Phi, 4 Az over El, 5 El over Az,
6 Az and El, 7 U-V contour 2
Enter Phi 0
Enter Theta Start,Stop,Step 0,90,5
List? y
```

Input pattern polarization first, followed by the type of output pattern. Inputs 3 - 7 generate output text files. Because a great circle pattern was selected, input of Phi plane is required, followed by pattern angles (Theta).

```
Phi =      0.00

Theta  Amplitude  Phase
0.00   4.86       11.35
5.00   4.83       12.66
10.00  4.79       16.01
15.00  4.82       19.80
20.00  4.95       22.12
25.00  5.09       21.81
30.00  5.18       18.82
35.00  5.18       13.89
40.00  5.06        8.04
45.00  4.77        2.17
50.00  4.27       -3.18
55.00  3.55       -7.76
60.00  2.61      -11.53
65.00  1.48      -14.54
70.00  0.25      -16.85
75.00 -0.98      -18.57
80.00 -2.05      -19.74
85.00 -2.80      -20.42
90.00 -3.07      -20.64

Plot 0 none, 1 polar, 2 rectangular 0
Pattern? n
Array Element Impedance versus Scan Angle? n
Another scan angle? n
Another array? n
```

**VDAIMC** generates HPGL output plots, an ASCII text file, which can be converted to other formats by third party routines.

If we have fully excited array, the program will compute the element impedance variation versus scanning the array in a Phi plane (Eq. 3-18). It is meaningless in this case.

The following illustrates using the matrix file output of the previous run. **VDAIMC** checks only for number of elements which must match the XADEF array file. Care must be taken to not change element positions which would make the impedance matrix invalid. Because single element currents are entered, the dimensions of the V-dipole are not required.

The run below does not apply mutual coupling effects and computes the single element pattern. The uncoupled single V-dipole has a gain of 6.64 dB. A comparison with the run above shows that coupling reduces boresight gain by 1.78 dB. A single element surrounded by an array of loaded element is used to compute or measure the element in an array, called the scan element

## Chapter 12 Phased Arrays

pattern (formally called active pattern).

```
C:\Phased_Array>vdaimc
Enter input: 0 keyboard, 1 file 0
Enter units: 1 in, 2 cm, 3 ft, 4 m 1
Enter array efficiency: 0 none, 1 uniform, 2 Tapered Distr. 0
Enter 1 to use previous matrix and inverse 1
Enter matrix file vds19m.dat
Enter element current file vds19m.cur
Enter Name of XADEF File vds19.arr
Change of distribution only? n
Write adjusted XADEF file with mutual coupling? n
Enter scan direction Theta, Phi 0,0
Include mutual coupling effects? n
Pattern? y
Enter Output Code:
    1 E Theta, 2 E Phi 3 RHC, 4 LHC, 5 Max. Lin., 6 Min. Lin.,
7 +45 Comp., 8 -45 Comp., 9 Power 1
Enter type <1> Conical, <2> Great Circle,
3 Theta Phi, 4 Az over El, 5 El over Az,
6 Az and El, 7 U-V contour 2
Enter Phi 0
Enter Theta Start,Stop,Step 0,90,5
List? y

Phi =      0.00

Theta  Amplitude  Phase
0.00   6.64       0.00
5.00   6.61       0.00
10.00  6.49         0.00
15.00  6.30         0.00
20.00  6.03         0.00
25.00  5.66         0.00
30.00  5.20         0.00
35.00  4.64         0.00
40.00  3.96         0.00
45.00  3.15         0.00
50.00  2.23         0.00
55.00  1.18         0.00
60.00  0.01         0.00
65.00 -1.25         0.00
70.00 -2.54         0.00
75.00 -3.79         0.00
80.00 -4.86         0.00
85.00 -5.60         0.00
90.00 -5.86         0.00
Plot 0 none, 1 polar, 2 rectangular 0
```

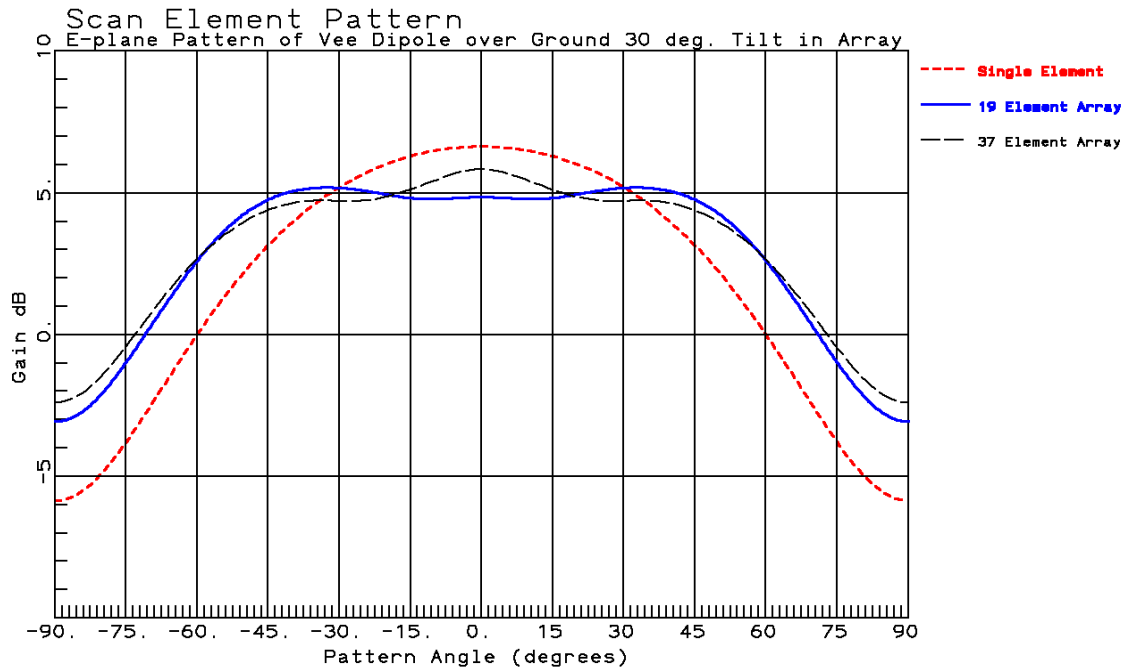


Figure 12-5.1.2 Center V-dipole in 19- and 37-element Hexagonal array spaced  $0.6\lambda$  on infinite ground plane *E*-plane Scan Element Pattern

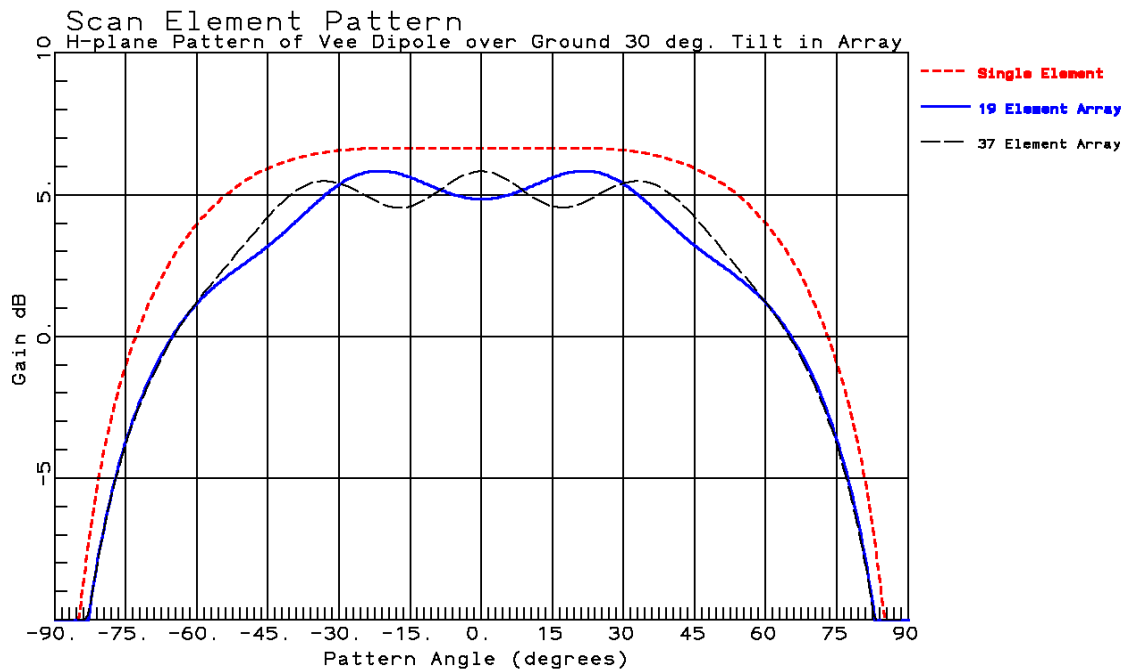
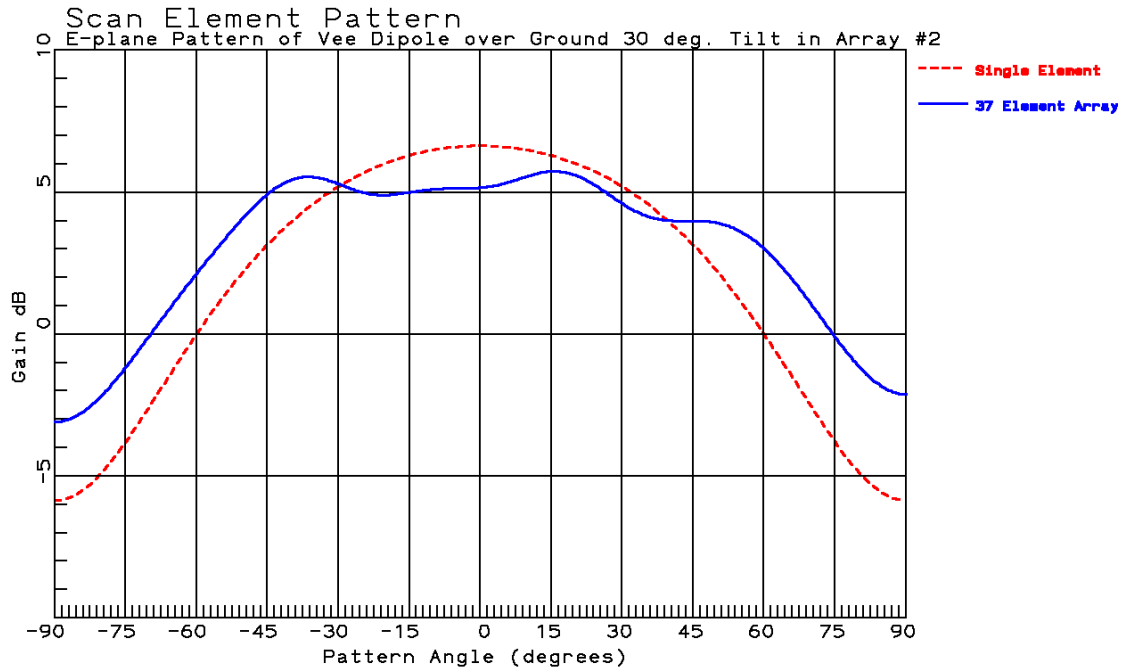
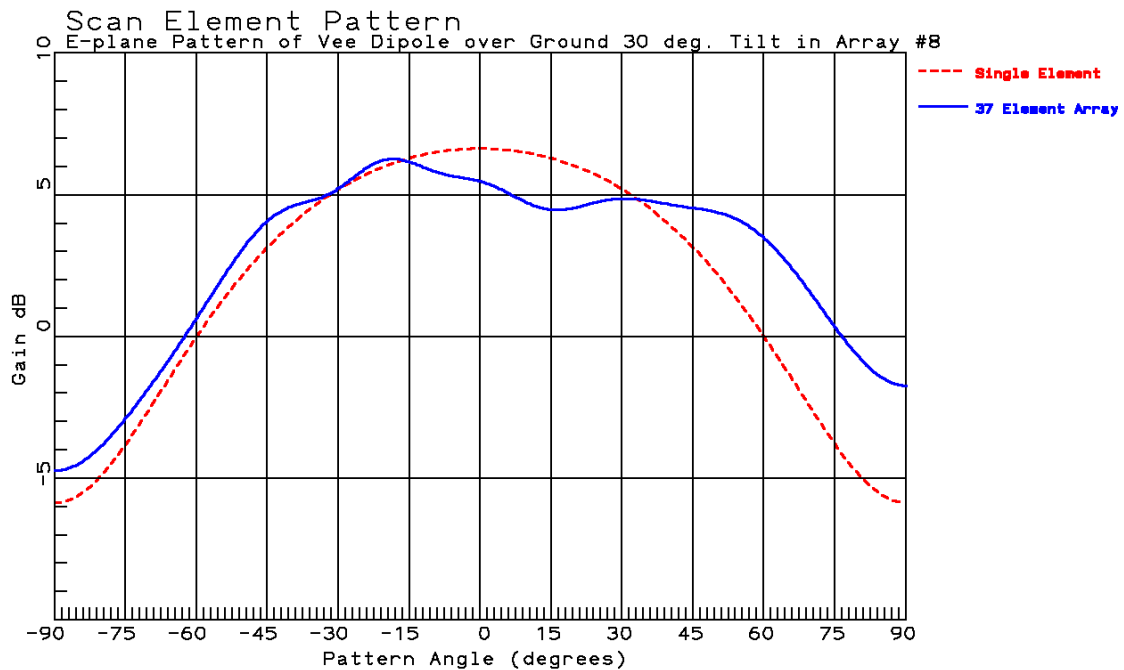


Figure 12-5.1.3 Center V-dipole in 19- and 37-element Hexagonal array spaced  $0.6\lambda$  on infinite ground plane *H*-plane Scan Element Pattern



**Figure 12-5.1.4 Element 2 V-dipole in 37-element Hexagonal array spaced  $0.6\lambda$  on infinite ground plane *E*-plane Scan Element Pattern**



**Figure 12-5.1.5 Element 8 V-dipole in 37-element Hexagonal array spaced  $0.6\lambda$  on infinite ground plane *E*-plane Scan Element Pattern**

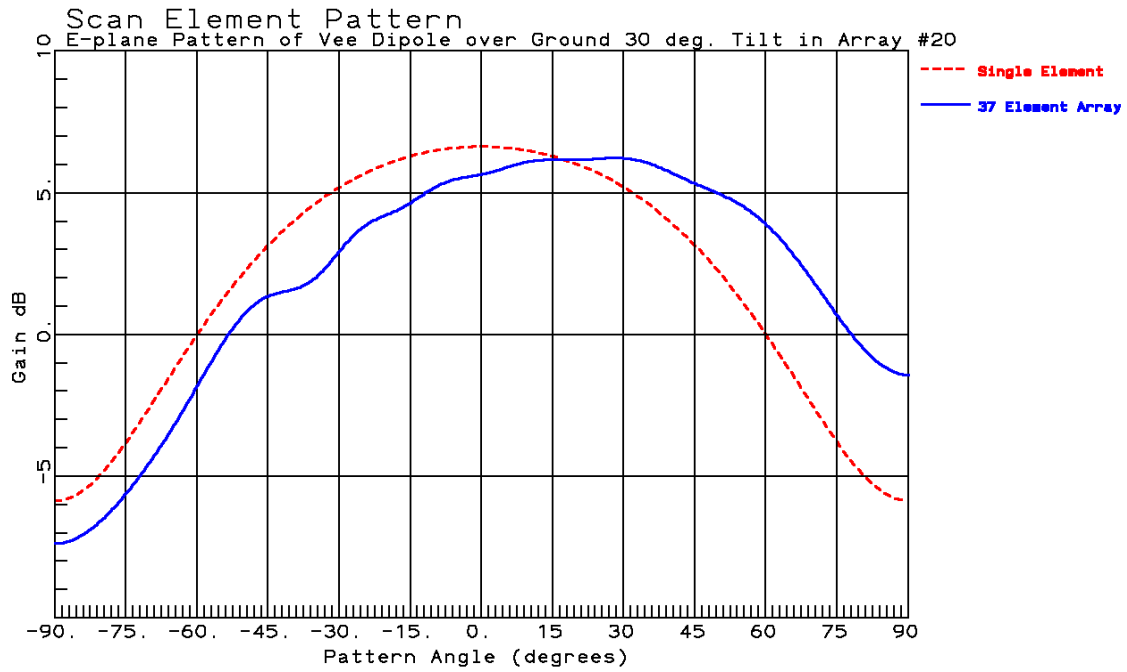


**Figure 12-5.1.6 Edge Element 20 V-dipole in 37-element Hexagonal array spaced  $0.6\lambda$  on infinite ground plane *E*-plane Scan Element Pattern**

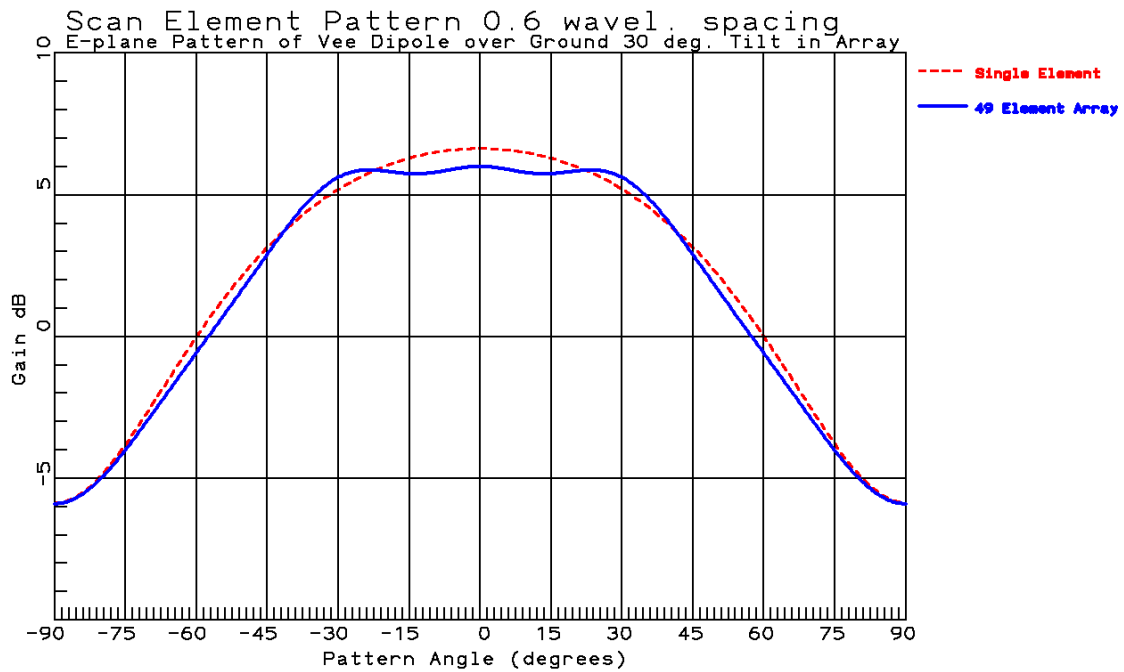


**Figure 12-5.1.7 Center V-dipole in 49-element Square array spaced  $0.6\lambda$  on infinite ground plane *E*-plane Scan Element Pattern**

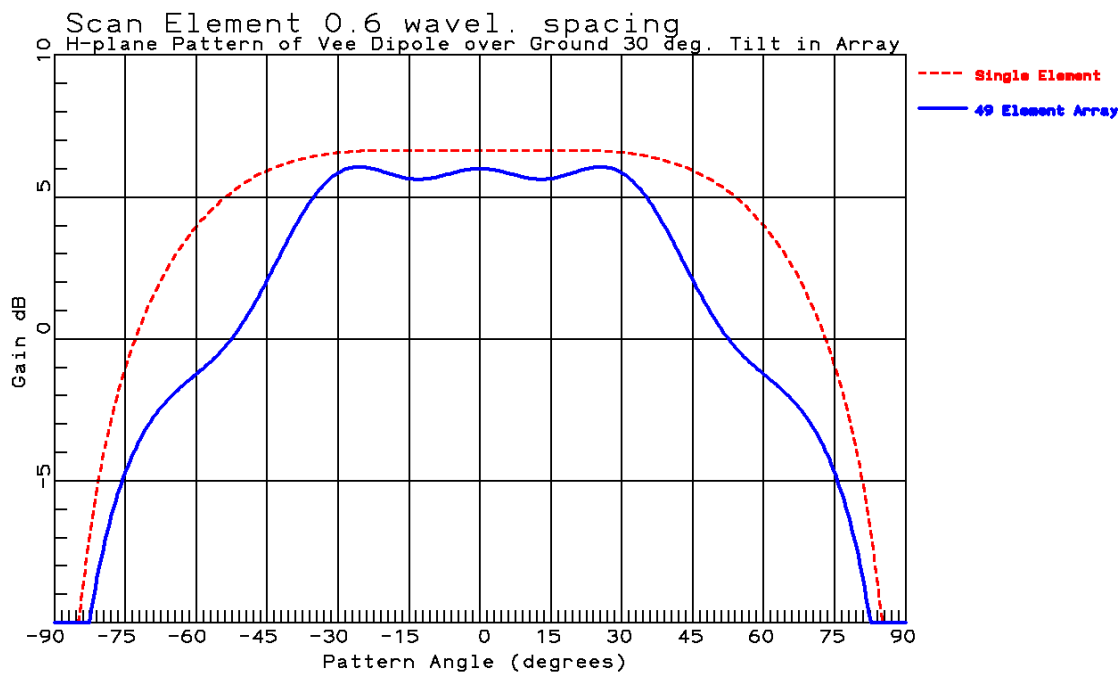


**Figure 12-5.1.8 Center V-dipole in 49-element Square array spaced  $0.6\lambda$  on infinite ground plane  $H$ -plane Scan Element Pattern**

Figures 7 and 8 show the scan element pattern for a center element located in a square ( $7 \times 7$ ) array with a  $0.6\lambda$  element spacing. Figure 8 has considerable pattern dip ( $45^\circ - 65^\circ$ ) for the embedded element compared to the single element. Pattern dips indicate scan angles where scan blindness occurs. However, a linear array with  $0.6\lambda$  spacing forms a grating lobe at about  $42^\circ$  so this pattern range would not be used. The hexagonal array with  $0.6\lambda$  element spacing does not form a grating lobe for scans in the  $E$ -plane. We eliminate grating lobes in linear arrays by using spacing elements of  $0.5\lambda$ .

Figures 9 and 10 predict that the gain of the center element falls 3.3 dB which means 53% of transmitter power reflects into the feed network. This un-radiated power is dissipated as heat which will raise the temperature until a thermo balance it reached. Over most scan angles the array approaches scan blindness. General practice is to look at the scan element pattern contour (U-V or Azimuth/Elevation), outputs of **VDAIMC**, to determine possible areas of scan blindness. High reflected power can lead to scan blindness. Whether it happens depends on the feed network interaction with the array (Section 11-7) including isolation levels between outputs.

The closely spaced elements in the array produces a higher change in the scan element pattern due to the higher element coupling. Each element has a different pattern (see Figures 2 - 6 above) which tends to average out the variations in the total pattern. Figures 11 and 12 show the computed pattern for a 49-element array spaced  $0.5\lambda$  where results illustrate pattern smoothing to nearly design results surprising because of the large change of the scan element pattern from the isolated element pattern (Figures 9 and 10). Results for  $0.6\lambda$  element spacing are similar. Figures 13 and 14 demonstrate that the LU decomposition works well for an array with 961 elements.

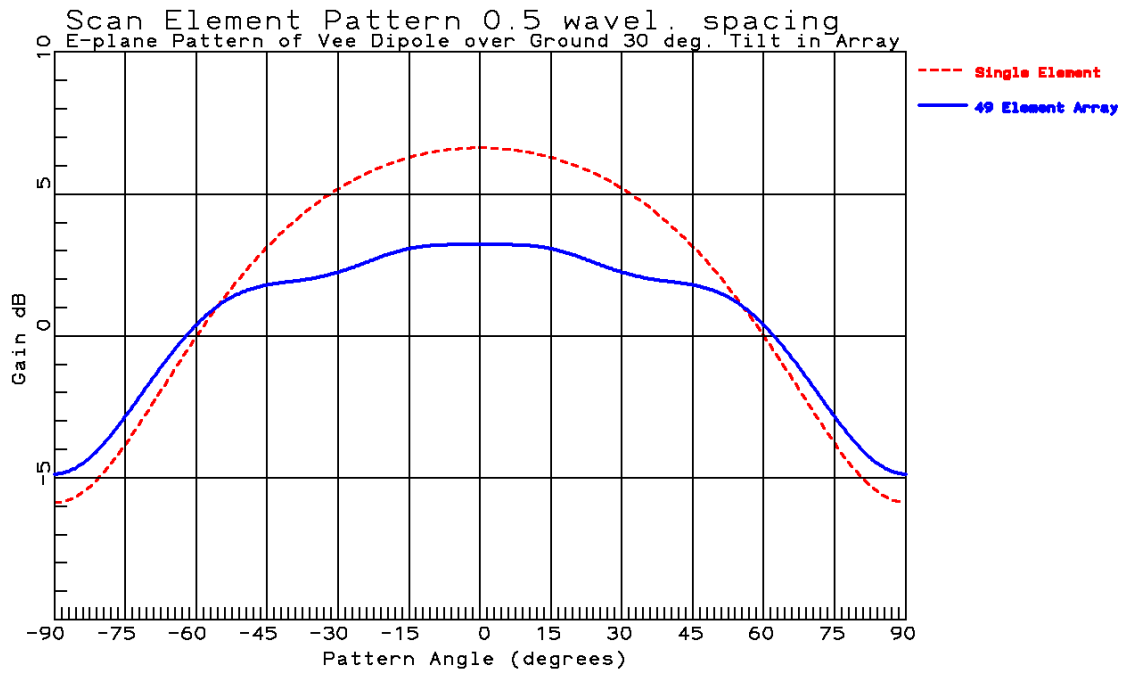


**Figure 12-5.1.9 Center V-dipole in 49-element Square array spaced  $0.5\lambda$  on infinite ground plane *E*-plane Scan Element Pattern**

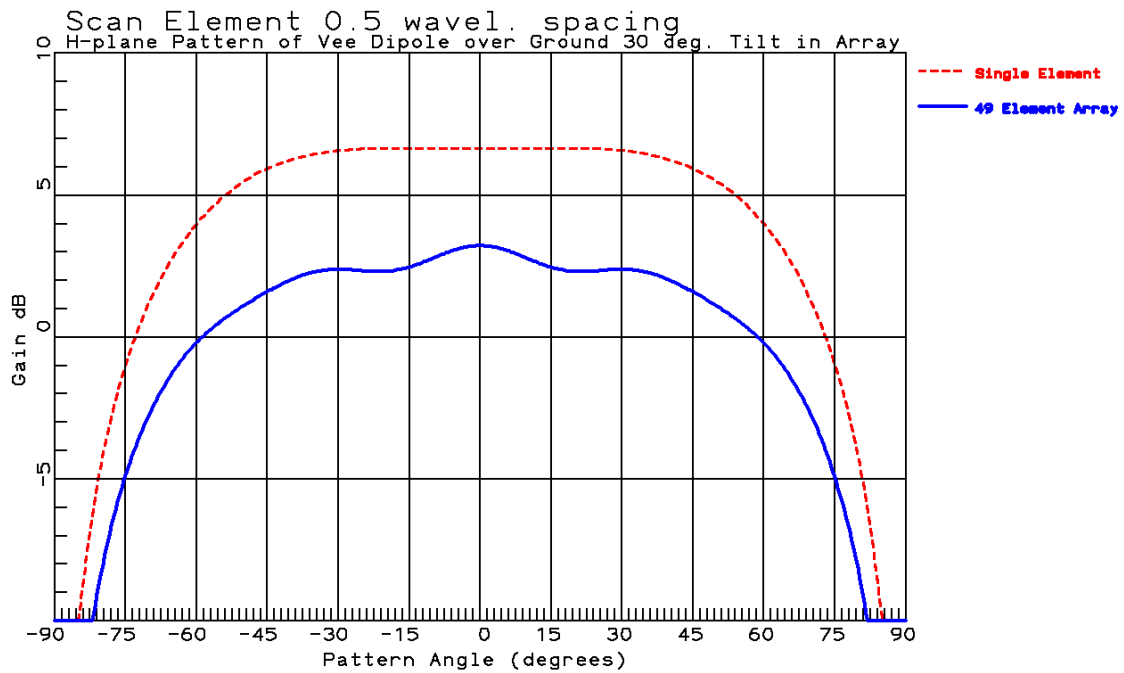


**Figure 12-5.1.10 Center V-dipole in 49-element Square array spaced  $0.5\lambda$  on infinite ground plane *H*-plane Scan Element Pattern**

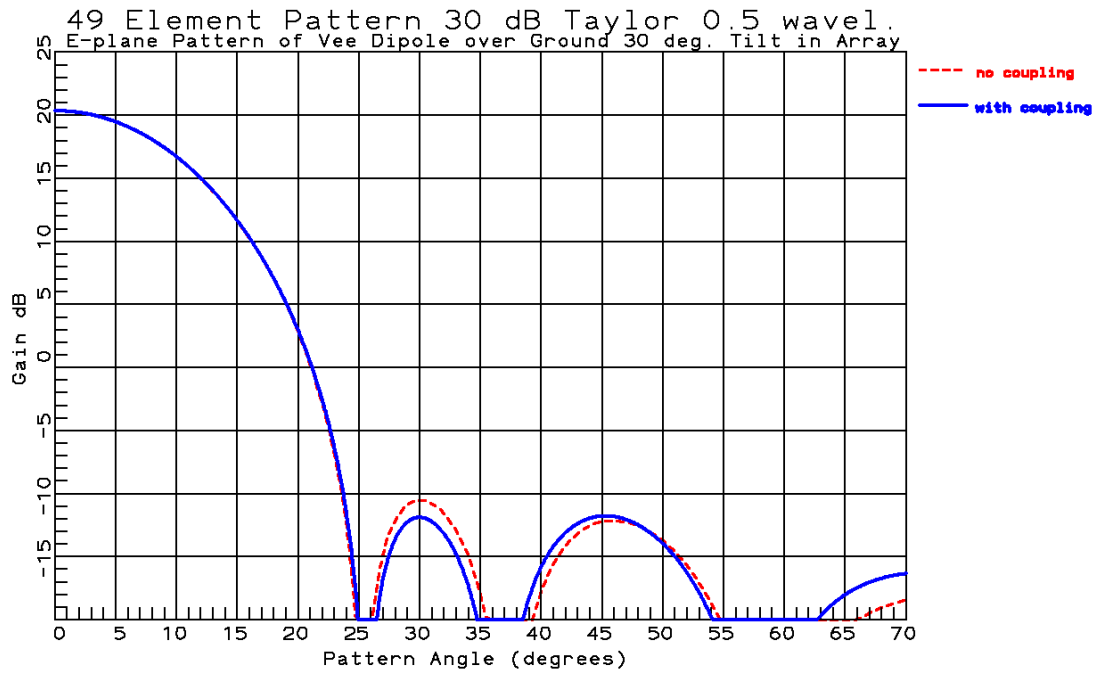


**Figure 12-5.1.11 V-dipole in 49-element Square array spaced  $0.5\lambda$  on infinite ground plane  $E$ -plane using zero sampled 30-dB Taylor distribution along both axes**

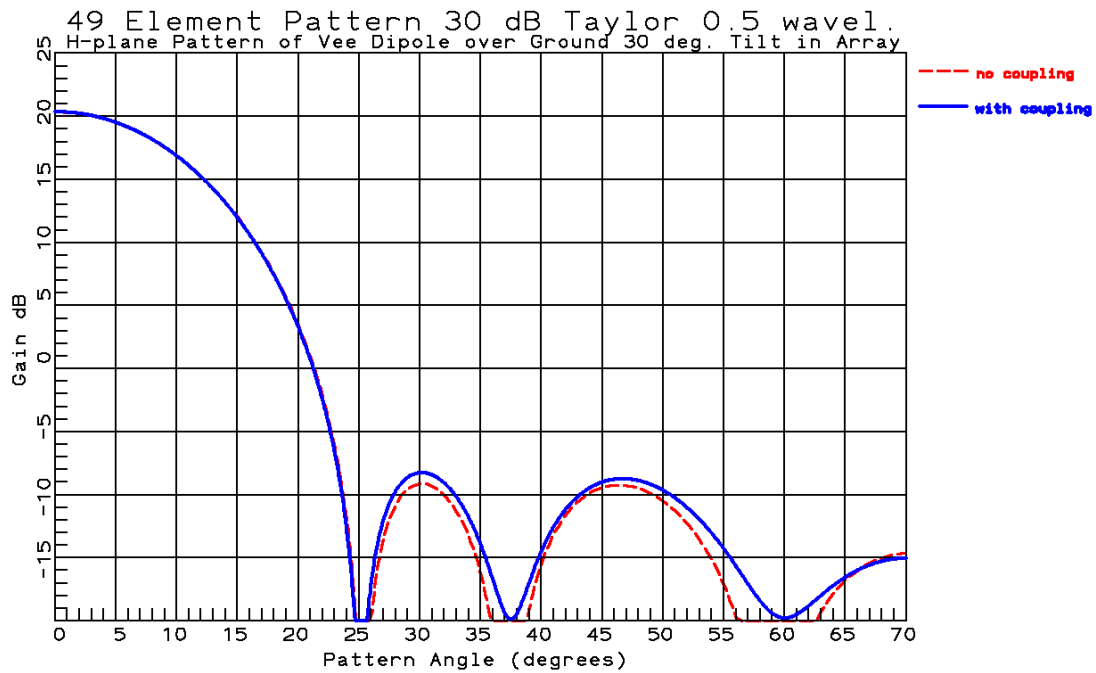


**Figure 12-5.1.12 V-dipole in 49-element Square array spaced  $0.5\lambda$  on infinite ground plane  $H$ -plane using zero sampled 30-dB Taylor distribution along both axes**

## Chapter 12 Phased Arrays

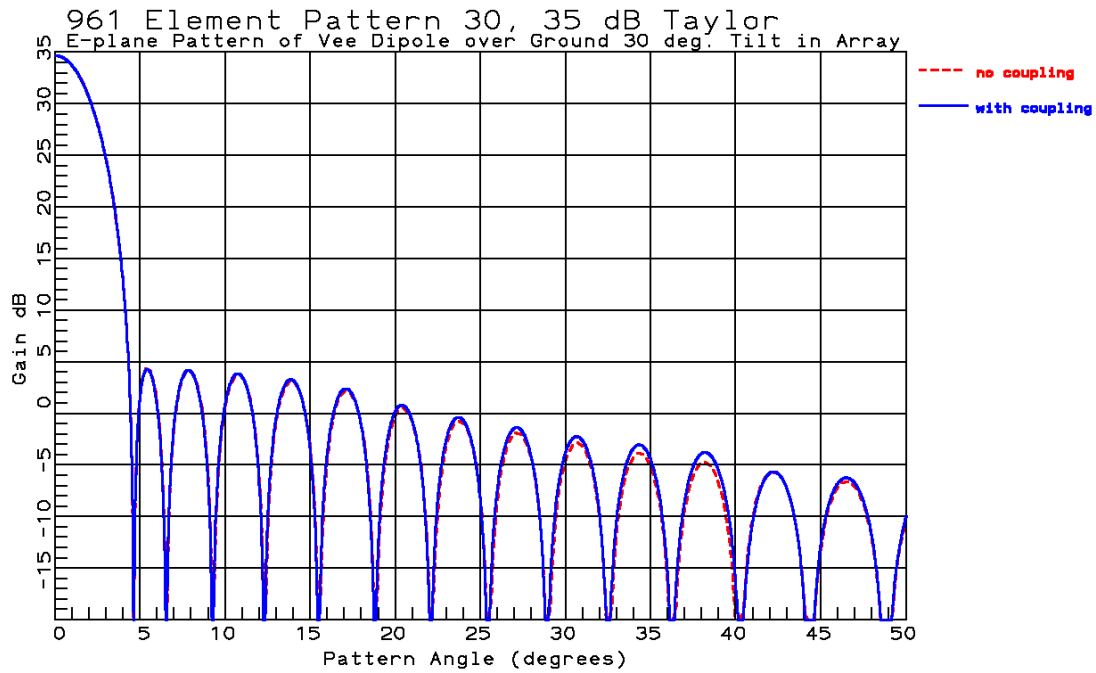


**Figure 12-5.1.13** V-dipole in 961-element Square array spaced  $0.6\lambda$  on infinite ground plane *E*-plane using zero sampled 30- and 35-dB Taylor distribution along x- and y-axes

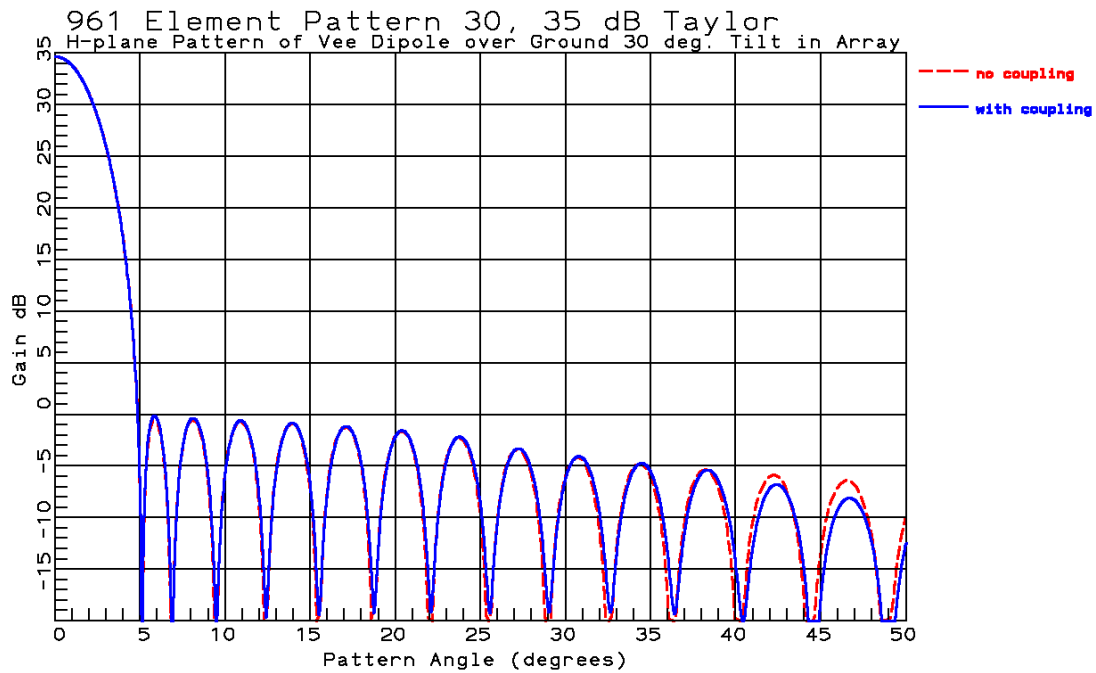


**Figure 12-5.1.14** V-dipole in 961-element Square array spaced  $0.6\lambda$  on infinite ground plane *H*-plane using zero sampled 30- and 35-dB Taylor distribution along x- and y-axes

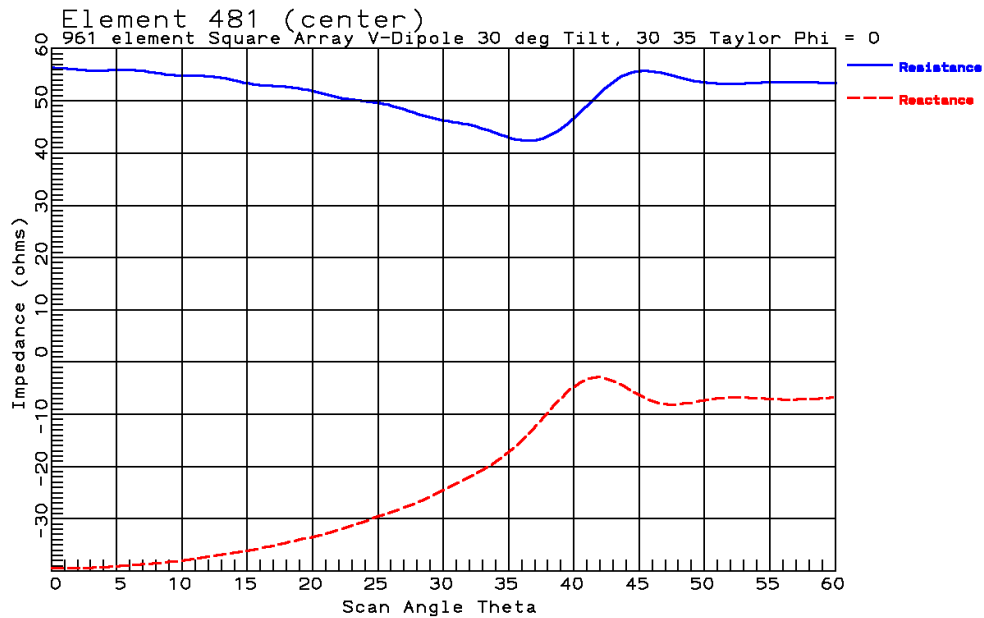


**Figure 12-5.1.15 V-dipole in 961-element Square array spaced  $0.6\lambda$  on infinite ground plane  $E$ -plane using zero sampled 30- and 35-dB Taylor distribution along x- and y-axes**

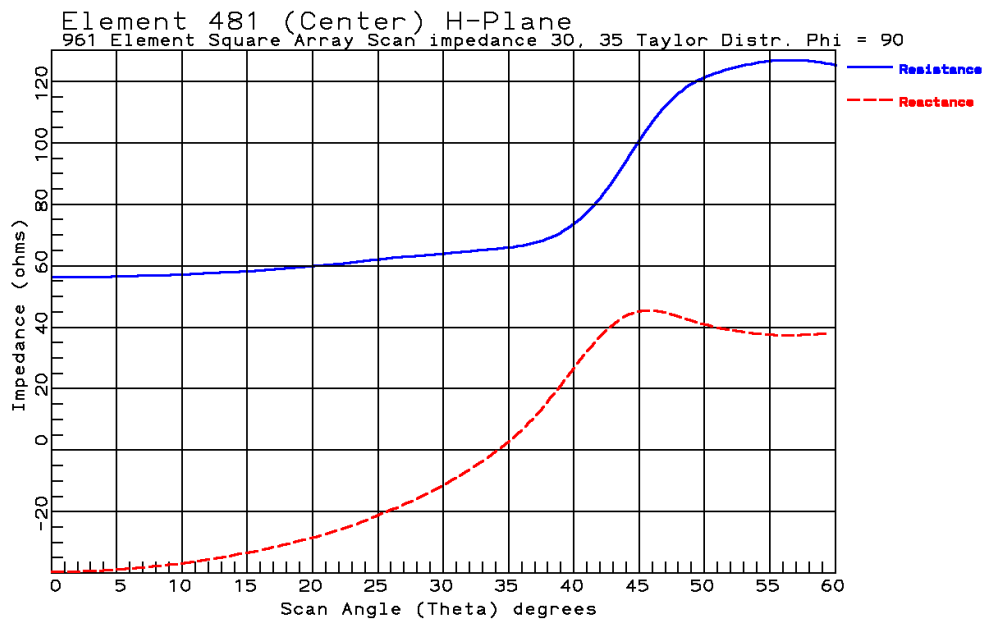


**Figure 12-5.1.16 V-dipole in 961-element Square array spaced  $0.6\lambda$  on infinite ground plane  $H$ -plane using zero sampled 30- and 35-dB Taylor distribution along x- and y-axes**

Figures 15 and 16 illustrate the array loaded impedance of the center element in the 961-element array. Note the  $H$ -plane has a rapid change near the angles where the grating lobe forms.

### Square Microstrip Patch Arrays

**SPAIMC** computes characteristics of square microstrip patches with the same capabilities as **VDAIMC**. Internally the program uses normalized mutual admittances similar to the results given in Section 6-10.1 Coupled Microstrip Patches. The form of the array element efficiency is similar to an array computed using impedance matrices.

$$Efficiency = \frac{\sum_{i=1}^N |E_i|^2}{\sum_{i=1}^N \sum_{j=1}^N \left[ \frac{G_{ij}}{G_{11}} \right] Re \left[ \frac{E_j}{E_i} \right] |E_i|^2}$$

The scan element pattern is computed for the center element in both 19- and 37-element hexagonal arrays and compared to the single element pattern.

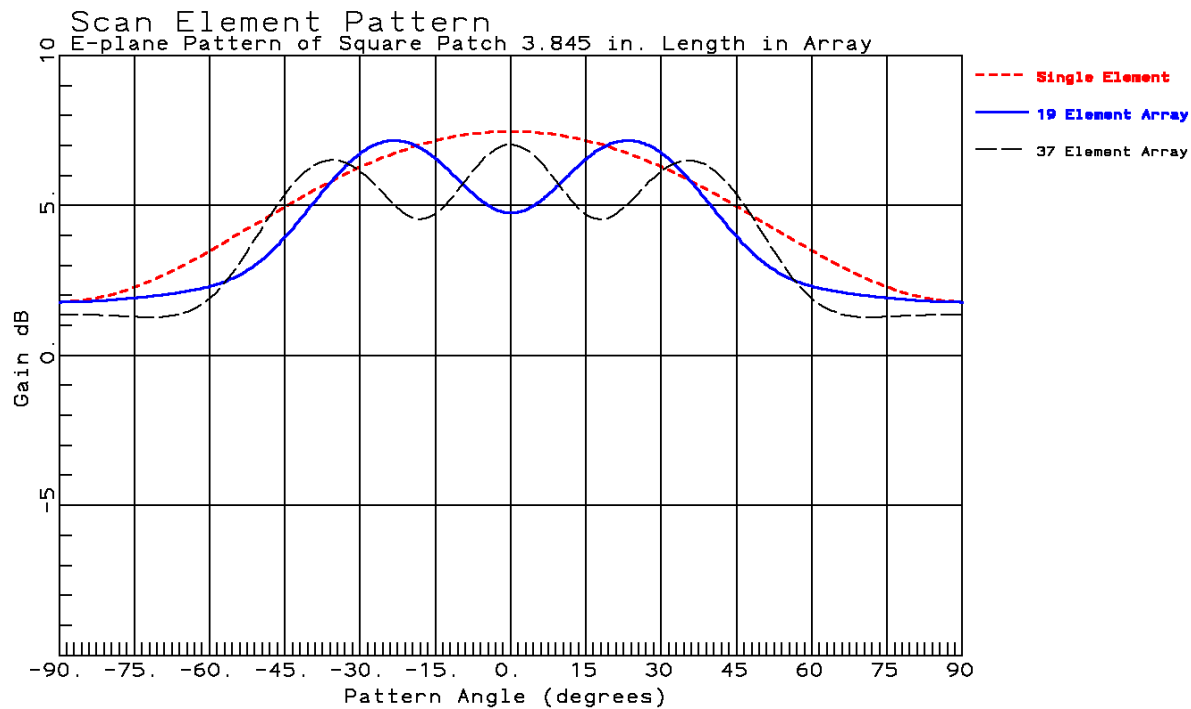


**Figure 12-5.1.17 Center Square Patch in 19- and 37-element Hexagonal array spaced  $0.6\lambda$  on infinite ground plane E-plane Scan Element Pattern**

The square patch scan element patterns are similar to the V-dipole except the variation is greater since the single element pattern gain is greater (7.48-dB versus 6.6-dB). The gain of the associated uniform distribution area is 4.68 dB for the hexagonal array with  $0.6\lambda$  spacing. A square array with  $0.6\lambda$  sides has an associated area gain of 6.56-dB and produces less scan element pattern ripple: Figures 20 and 21

The edge scan element pattern (#20) computed for the square patch, Figure 19, is similar to Figure 6 of the V-dipole.

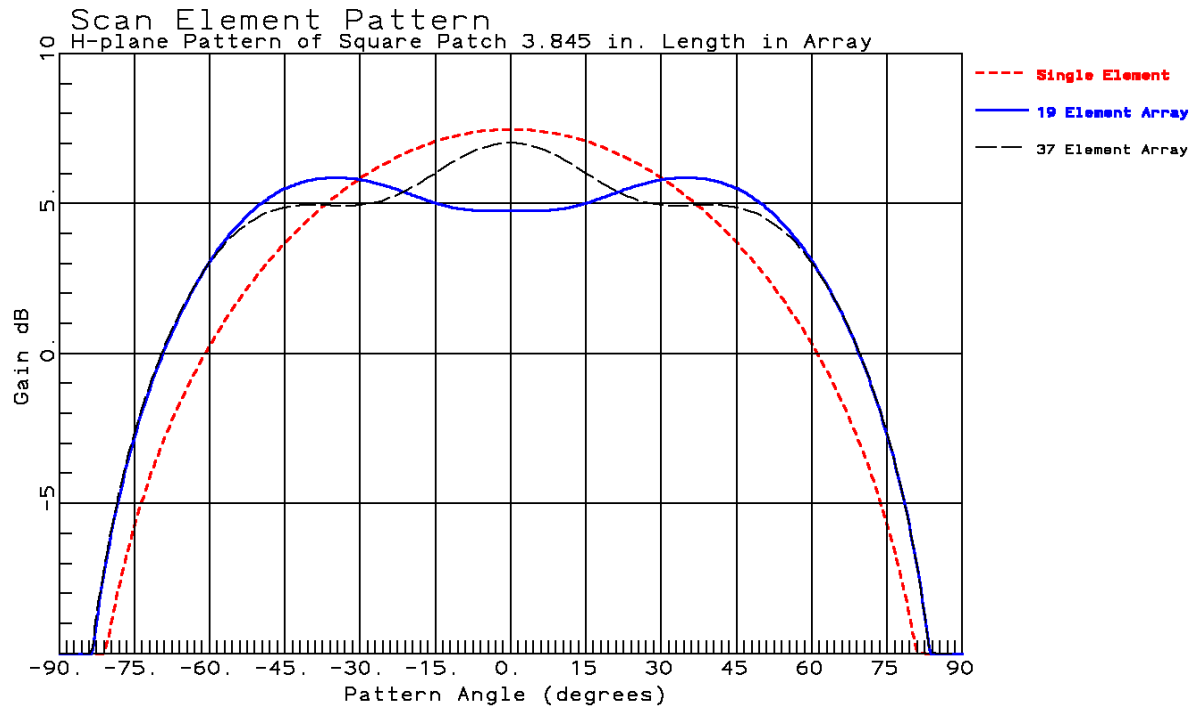


**Figure 12-5.1.18 Center Square Patch in 19- and 37-element Hexagonal array spaced  $0.6\lambda$  on infinite ground plane  $H$ -plane Scan Element Pattern**

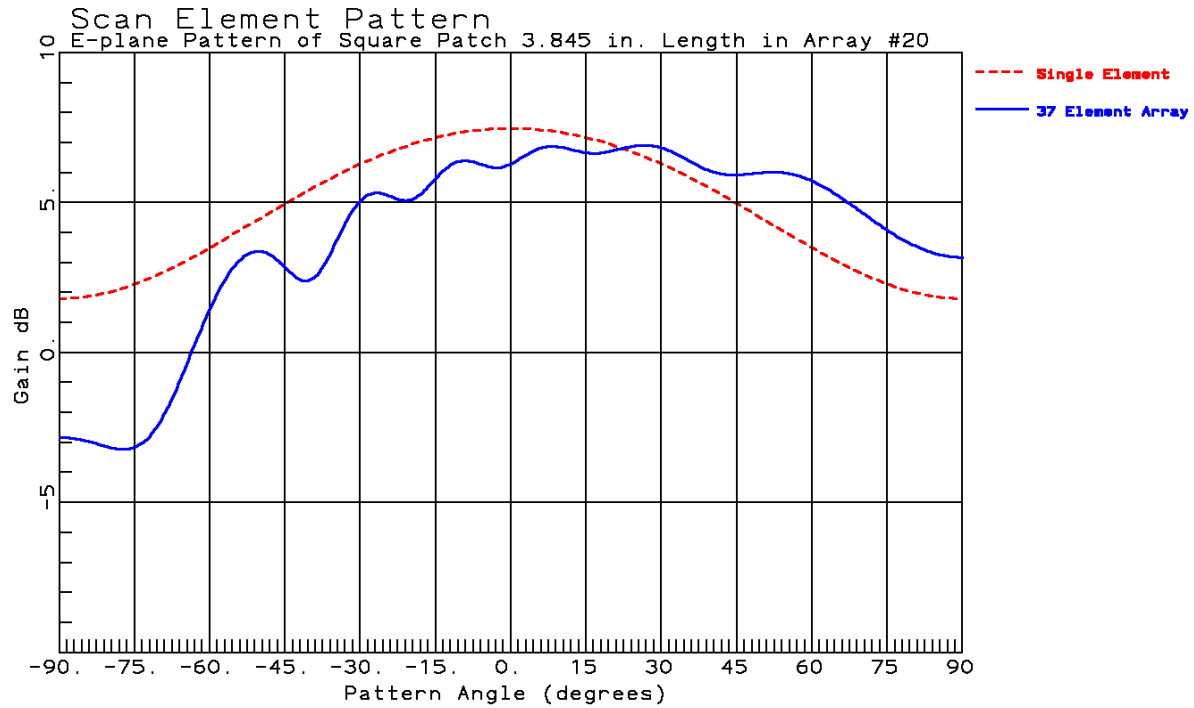


**Figure 12-5.1.19 Edge Element 20 Square Patch in 37-element Hexagonal array spaced  $0.6\lambda$  on infinite ground plane  $E$ -plane Scan Element Pattern**

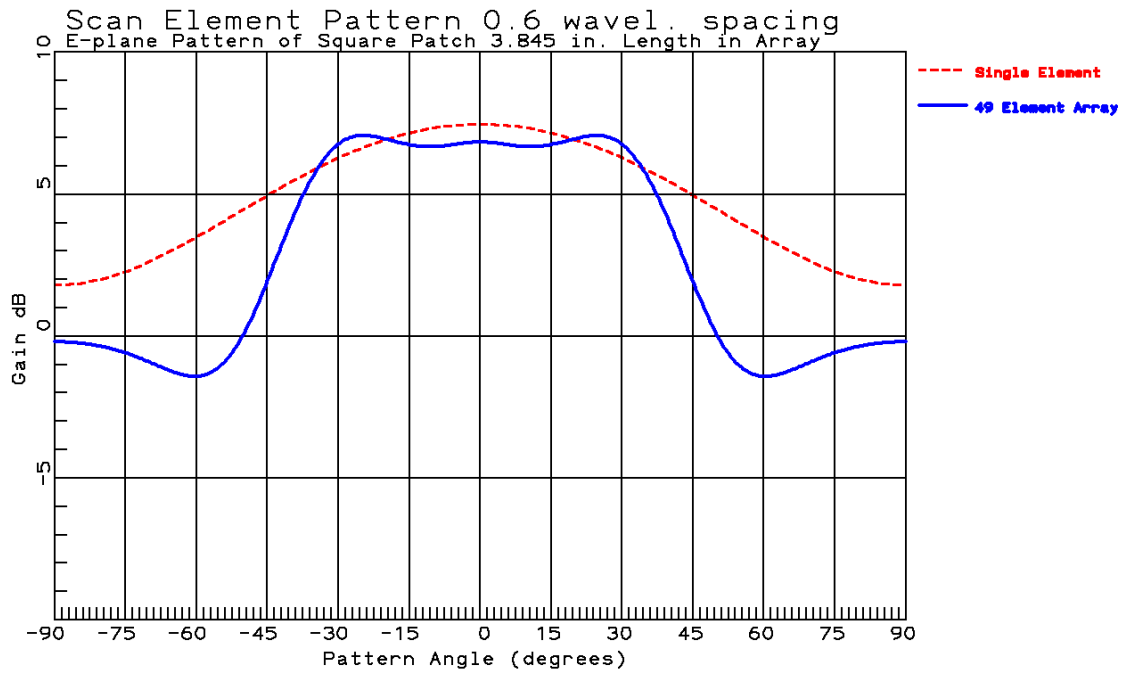


**Figure 12-5.1.20 Center Square Patch in 49-element Square array spaced  $0.6\lambda$  on infinite ground plane *E*-plane Scan Element Pattern**

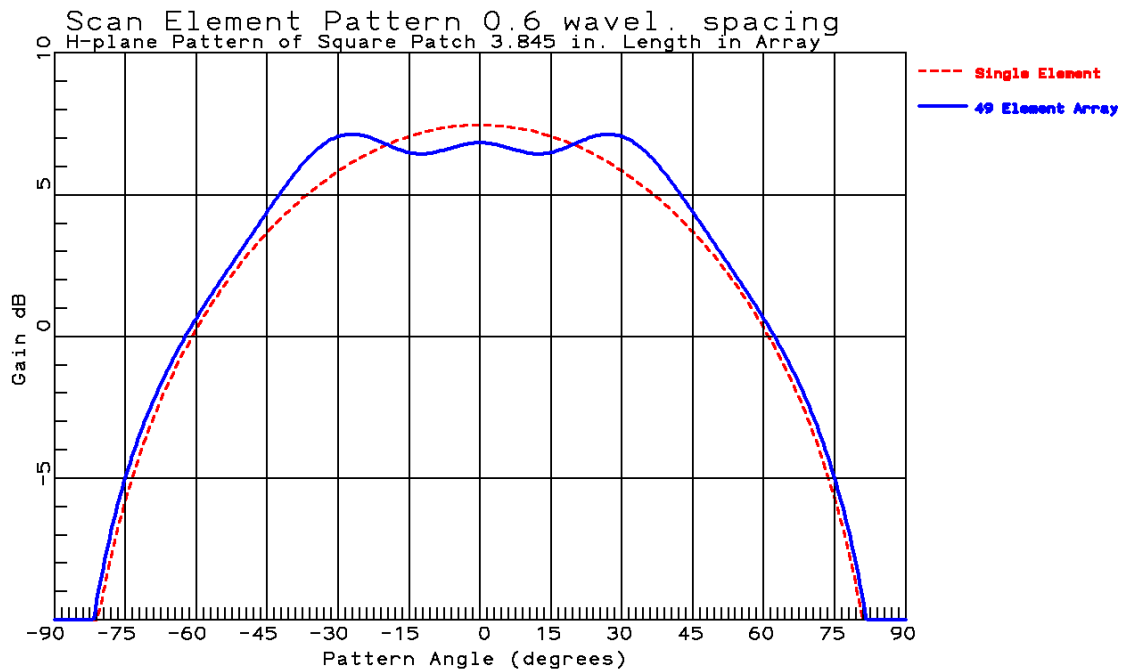


**Figure 12-5.1.21 Center Square Patch in 49-element Square array spaced  $0.6\lambda$  on infinite ground plane *H*-plane Scan Element Pattern**

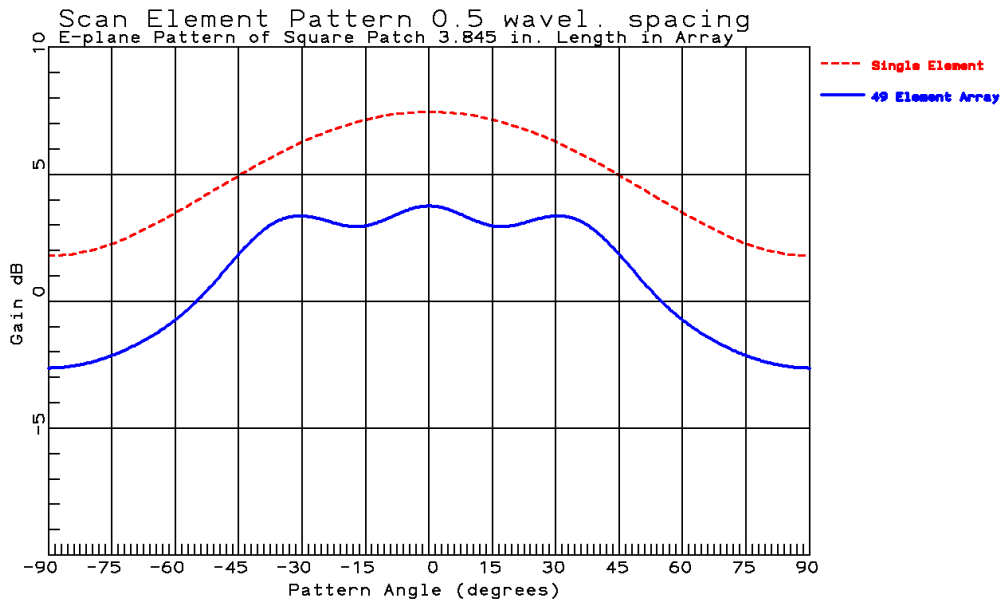


**Figure 12-5.1.22 Center Square Patch in 49-element Square array spaced  $0.5\lambda$  on infinite ground plane *E*-plane Scan Element Pattern**

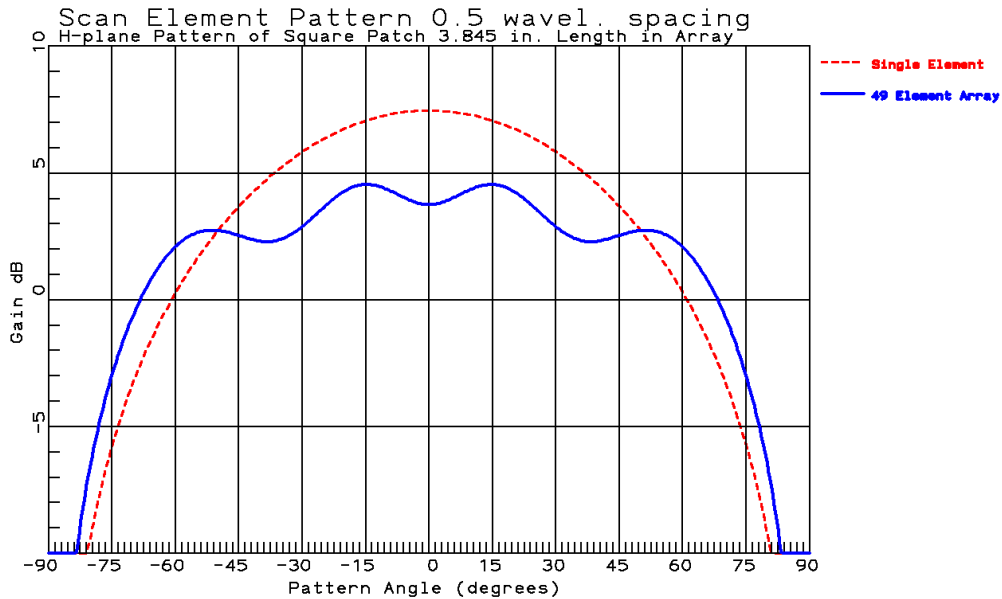


**Figure 12-5.1.23 Center Square Patch in 49-element Square array spaced  $0.5\lambda$  on infinite ground plane *E*-plane Scan Element Pattern**

Similar to the V-dipole in a  $0.5\lambda$  spaced square array, a square patch array reflects 60% of the transmit power dissipated as heat in the feed network or appears as an input mismatch. High reflected power can lead to scan blindness. Whether it happens depends on the feed network interaction with the array (Section 11-7) including isolation levels between outputs.

## Chapter 12 Phased Arrays

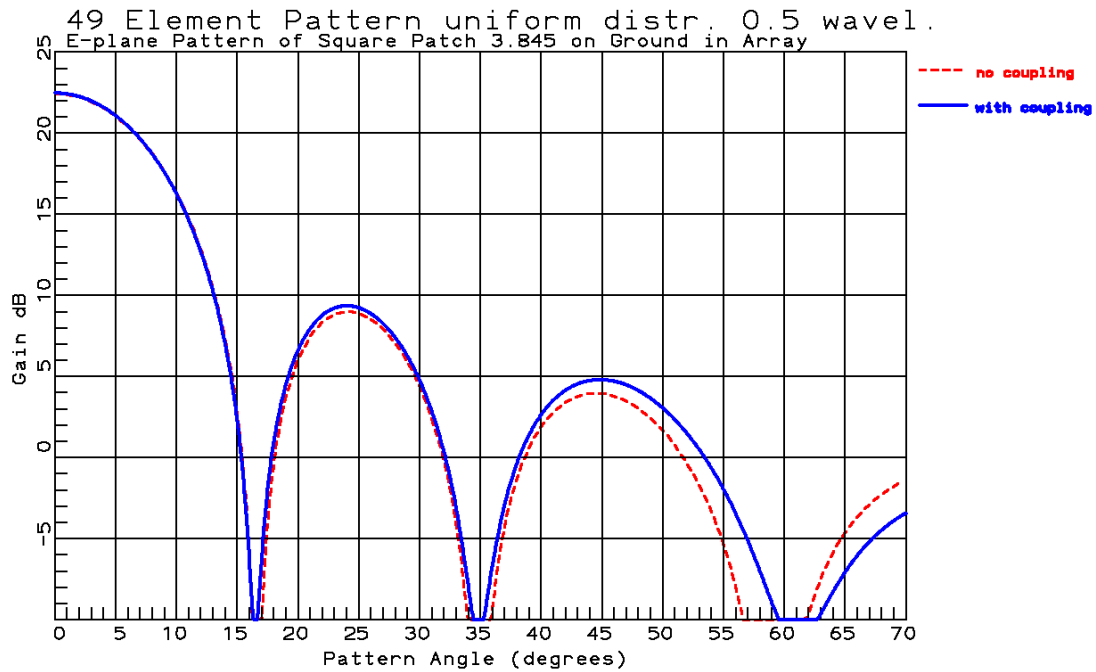


**Figure 12-5.1.24 49-element with Uniform Distribution Square array of Square Patches spaced  $0.5\lambda$   $E$ -plane**

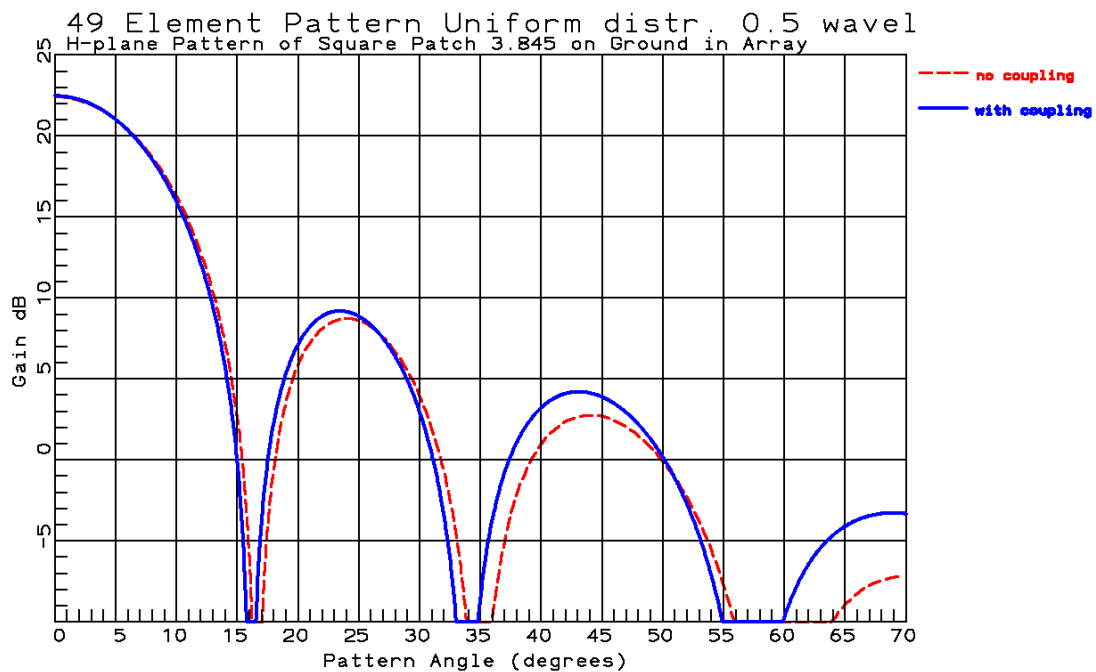


**Figure 12-5.1.25 49-element with Uniform Distribution Square array of Square Patches spaced  $0.5\lambda$   $H$ -plane**

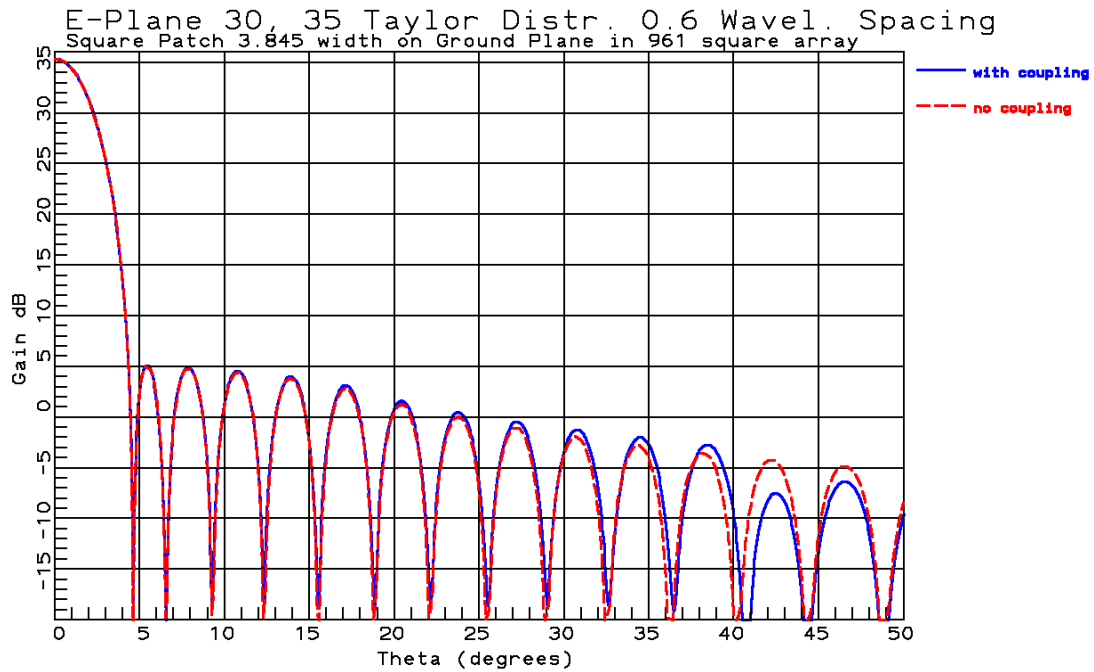


Figure 12-5.1.26 Square Patch in 961-element Square array spaced  $0.6\lambda$  on infinite ground plane  $E$ -plane using zero sampled 30- and 35-dB Taylor distribution along x- and y-axes

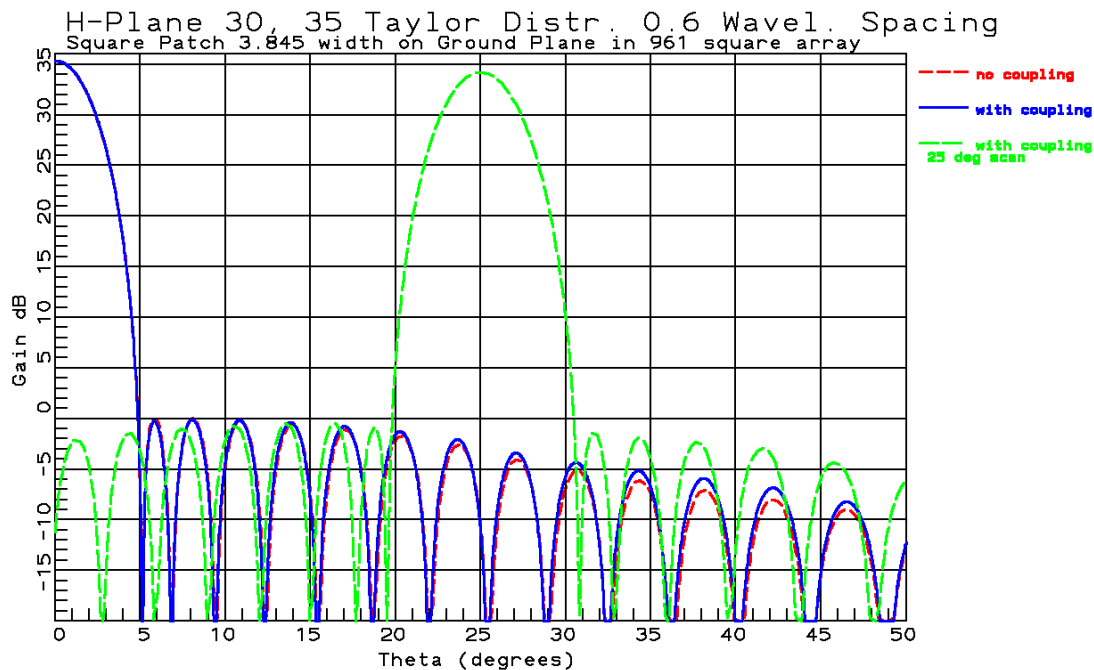
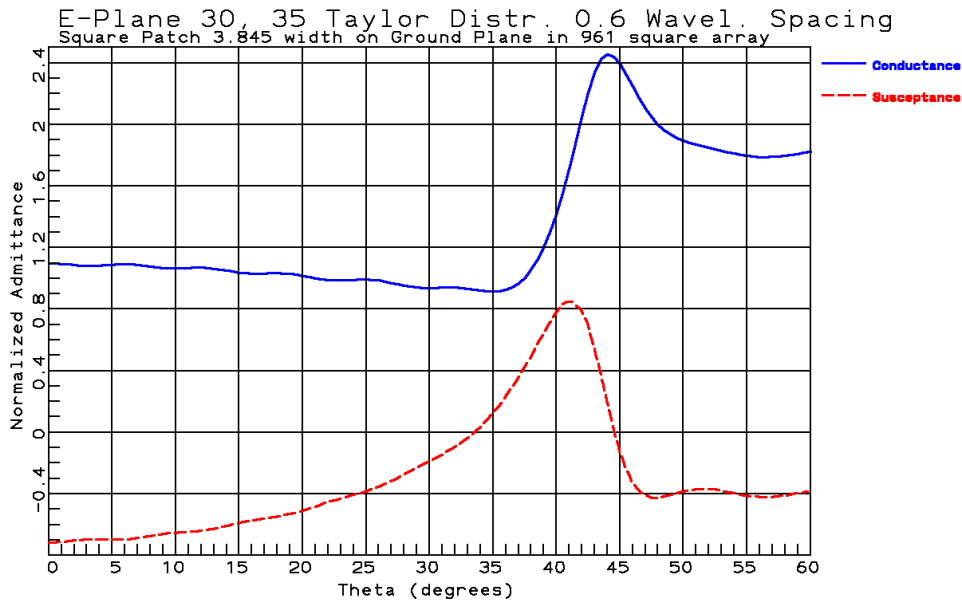
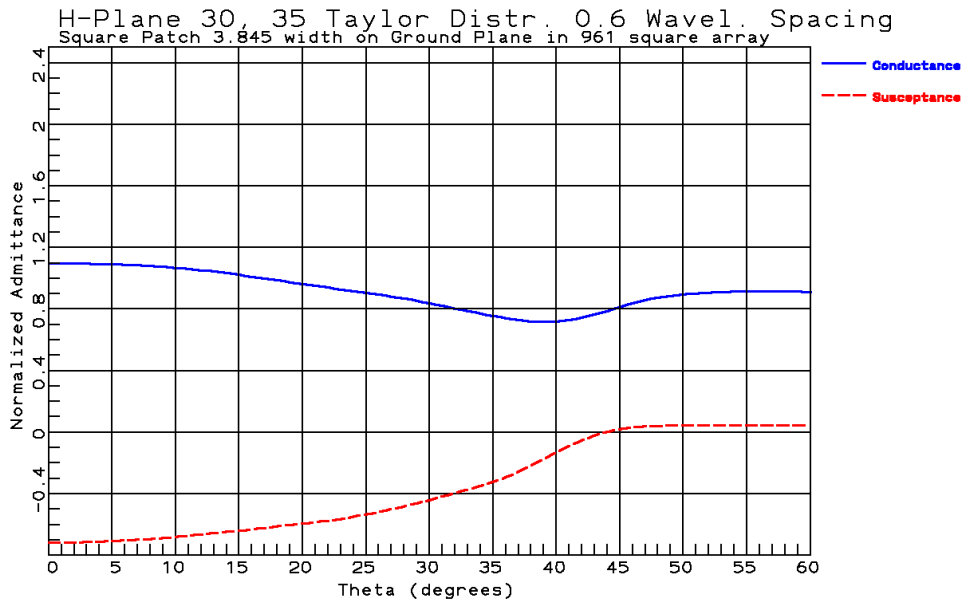


Figure 12-5.1.27 Square Patch in 961-element Square array spaced  $0.6\lambda$  on infinite ground plane  $E$ -plane using zero sampled 30- and 35-dB Taylor distribution along x- and y-axes



**Figure 12-5.1.28 Square Patch in 961-element Square array spaced  $0.6\lambda$  on infinite ground plane  $E$ -plane using zero sampled 30- and 35-dB Taylor distribution along x- and y-axes**



**Figure 12-5.1.29 Square Patch in 961-element Square array spaced  $0.6\lambda$  on infinite ground plane  $E$ -plane using zero sampled 30- and 35-dB Taylor distribution along x- and y-axes**

Figures 28 and 29 show the normalized admittance of the center element (481) in the 961-element array spaced  $0.6\lambda$ . The admittance changes rapidly as the grating lobe angle is approached ( $42^\circ$ ) in the square  $0.6\lambda$  spaced array.

**CPAIMC** and **RPAIMC** are similar programs for circular and rectangular patches

## V-dipole array on Polygon Ground Plane

A real array is mounted on a finite ground plane. Physical optics can be used to predict the effect of a polygon shaped ground plane. The finite size of the ground plane changes mutual impedances little, but will introduce pattern ripple. This ripple makes direct measurement of scan element pattern difficult. **VDAIMCP** includes PO analysis of an array mounted over a polygon shaped ground plane. Mutual impedance computations use image dipoles, but only the real dipole radiation is used to compute ground plane currents. A hexagonal ground plane extending one  $\lambda$  beyond the extent of the 37-element hexagonal array of V-dipoles gives the following scan element patterns

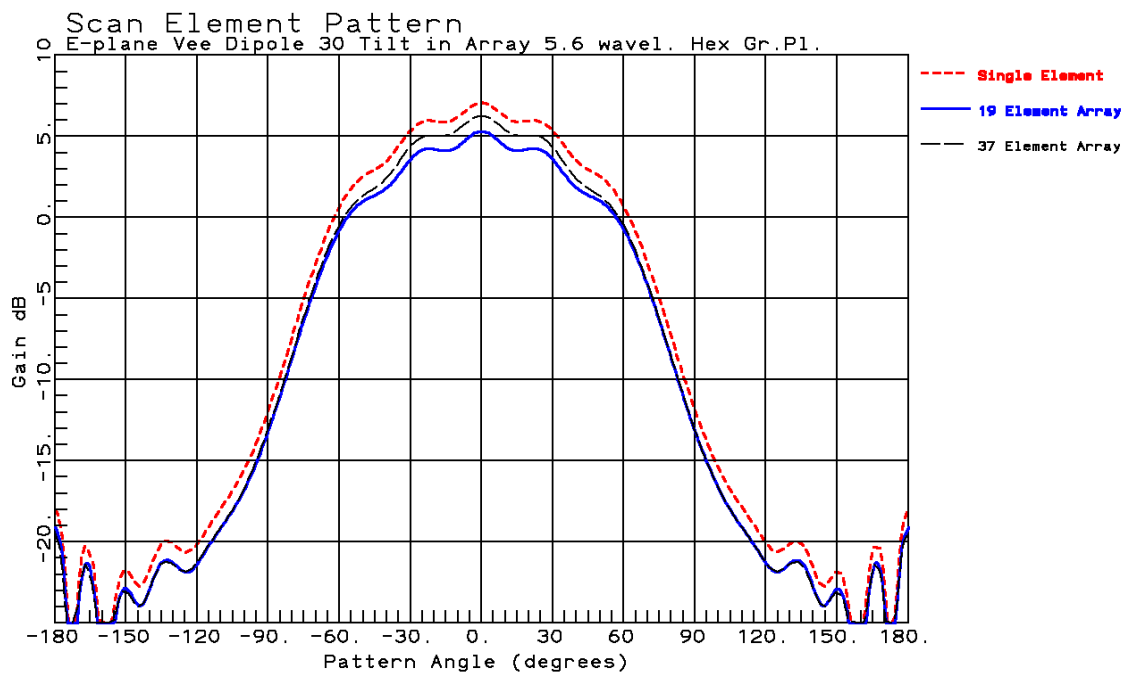


**Figure 12-5.1.30 E-Plane Scan Element Pattern of Center element V-dipole in 19- and 37-element hexagonal array spaced  $0.6\lambda$  mounted on  $5.6\lambda$  ground plane**

To make a direct comparison with Figures 2 and 3, these complete patterns showing the backlobe have been restricted to  $\pm 90^\circ$  in Figures 32 and 33. The finite ground plane lowers the *E*-plane pattern to -13 dB at  $90^\circ$ . An infinite ground plane produces an *H*-plane null whereas the finite ground plane can only reduce the pattern to  $\sim -10$  dB.

The finite ground plane modifies the rippled pattern of off-center elements. Figure 34 with only one  $\lambda$  ground plane on positive  $\theta$  side fails to support the pattern shown in Figure 6. Figures 35 and 36 show how extending the ground plane  $5\lambda$  beyond the outer elements decreases the backlobe and increases the main beam ripple rate. The *E*-plane pattern level at  $90^\circ$  is similar with either ground plane while the *H*-plane level drops about 5 dB.

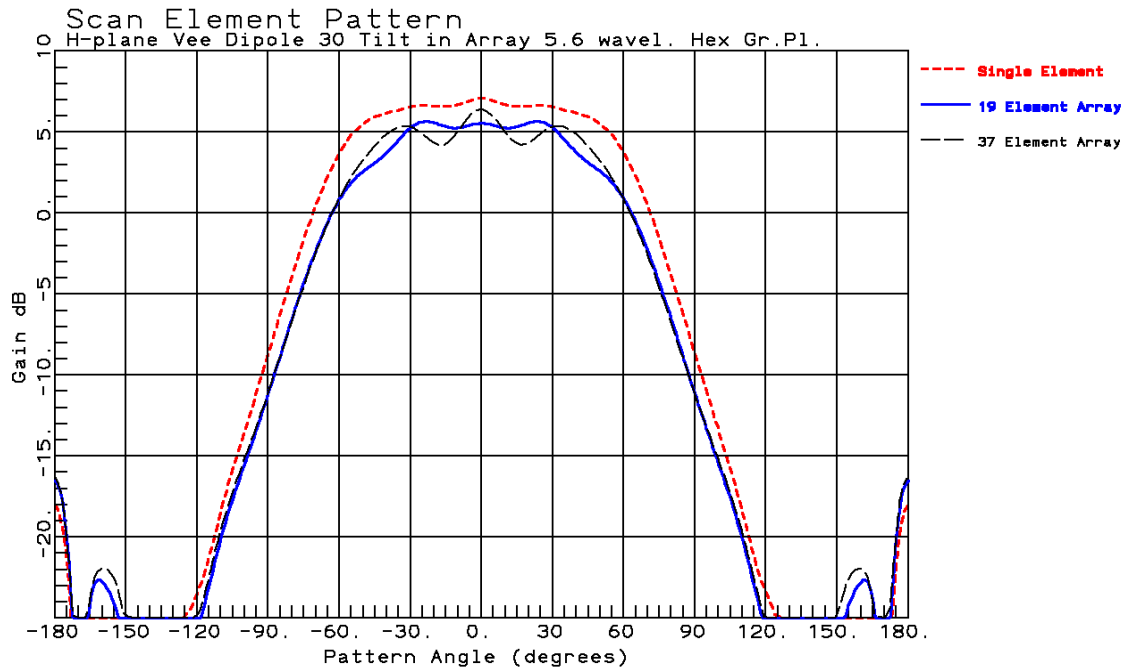


**Figure 12-5.1.31 H-Plane Scan Element Pattern of Center element V-dipole in 19- and 37-element hexagonal array spaced  $0.6\lambda$  mounted on  $5.6\lambda$  ground plane**

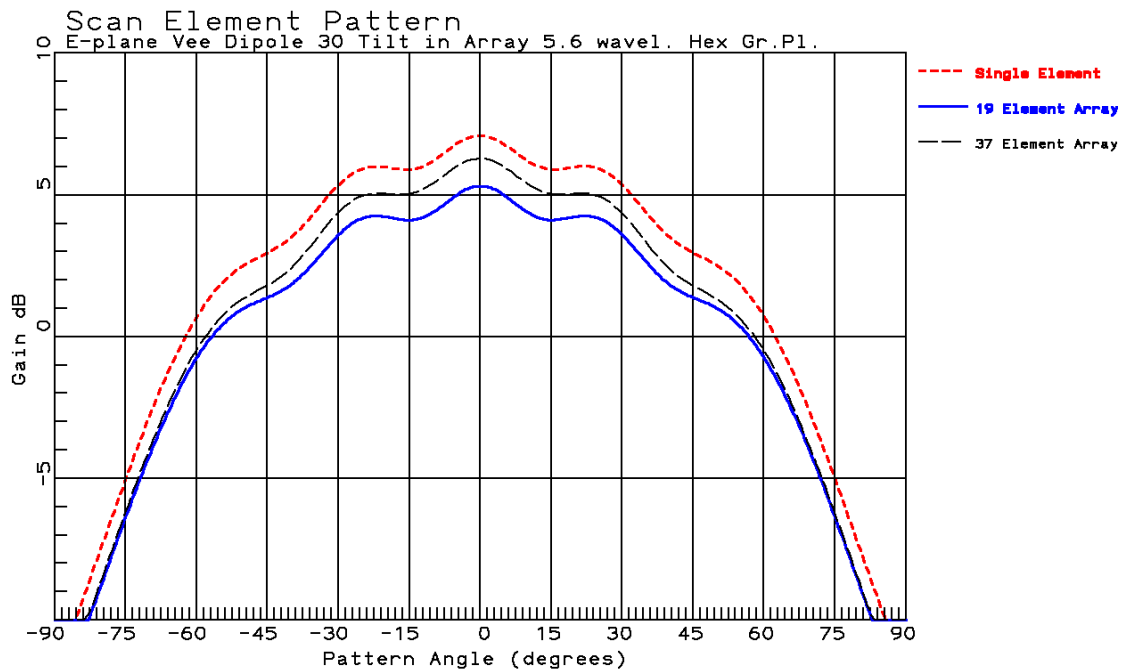


**Figure 12-5.1.32 E-Plane Scan Element Pattern of Center element V-dipole in 19- and 37-element hexagonal array spaced  $0.6\lambda$  mounted on  $5.6\lambda$  ground plane**

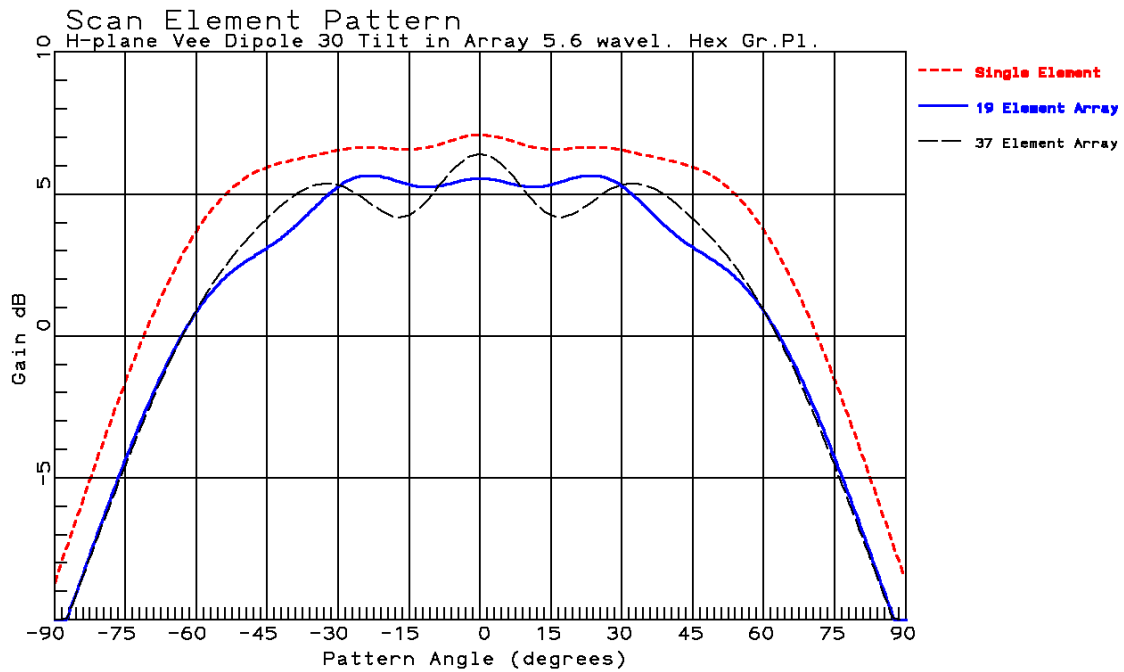


**Figure 12-5.1.33 H-Plane Scan Element Pattern of Center element V-dipole in 19- and 37-element hexagonal array spaced  $0.6\lambda$  mounted on  $5.6\lambda$  ground plane**

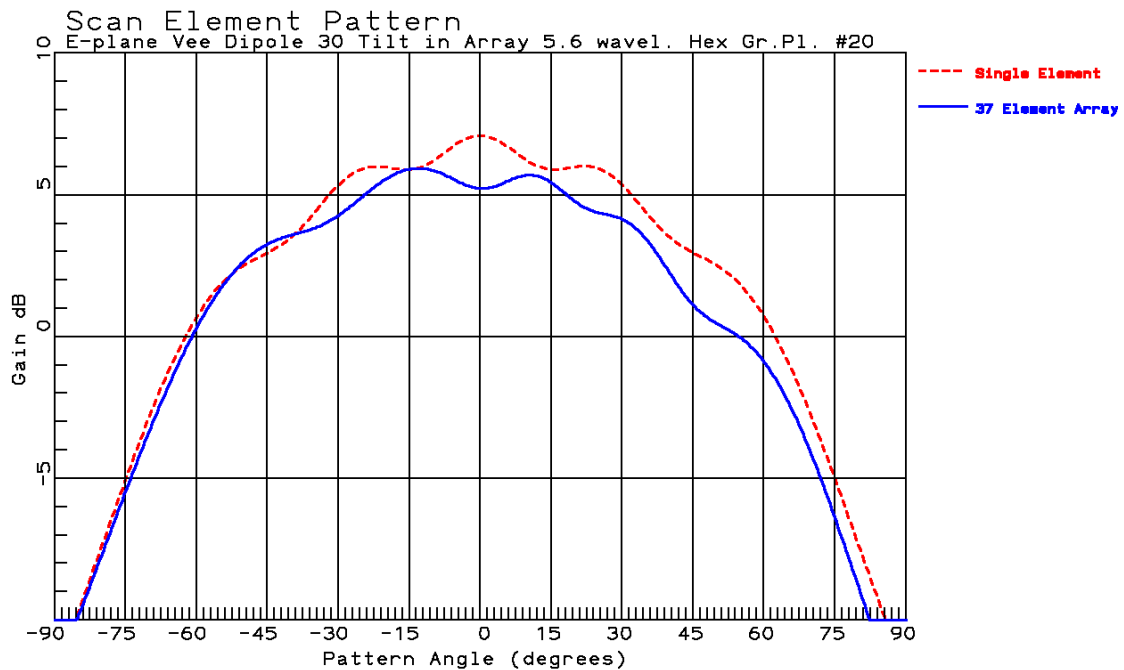


**Figure 12-5.1.34 E-Plane Scan Element Pattern of Edge element V-dipole in 19- and 37-element hexagonal array spaced  $0.6\lambda$  mounted on  $5.6\lambda$  ground plane**

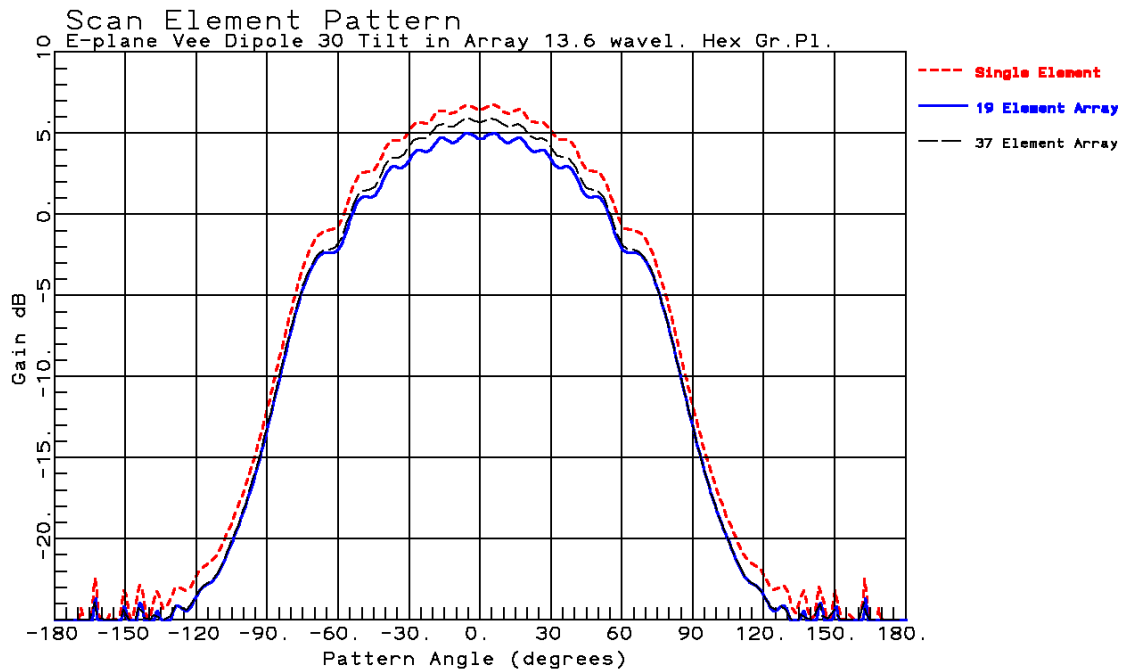


**Figure 12-5.1.35 E-Plane Scan Element Pattern of Center element V-dipole in 19- and 37-element hexagonal array spaced  $0.6\lambda$  mounted on  $13.6\lambda$  ground plane**

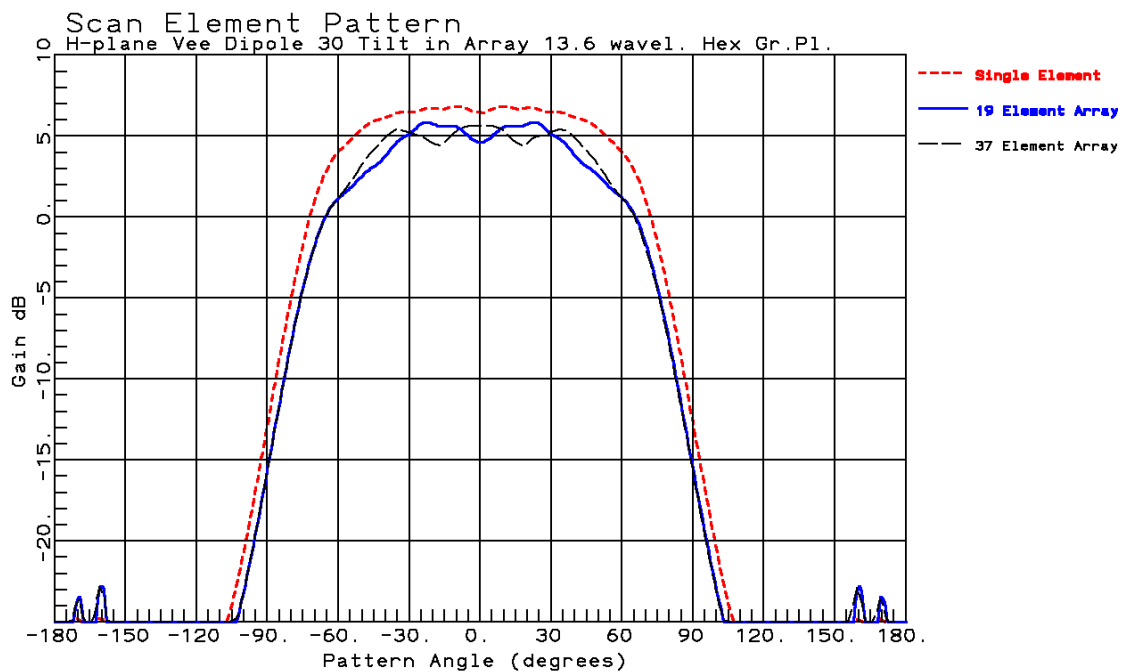


**Figure 12-5.1.36 H-Plane Scan Element Pattern of Center element V-dipole in 19- and 37-element hexagonal array spaced  $0.6\lambda$  mounted on  $13.6\lambda$  ground plane**

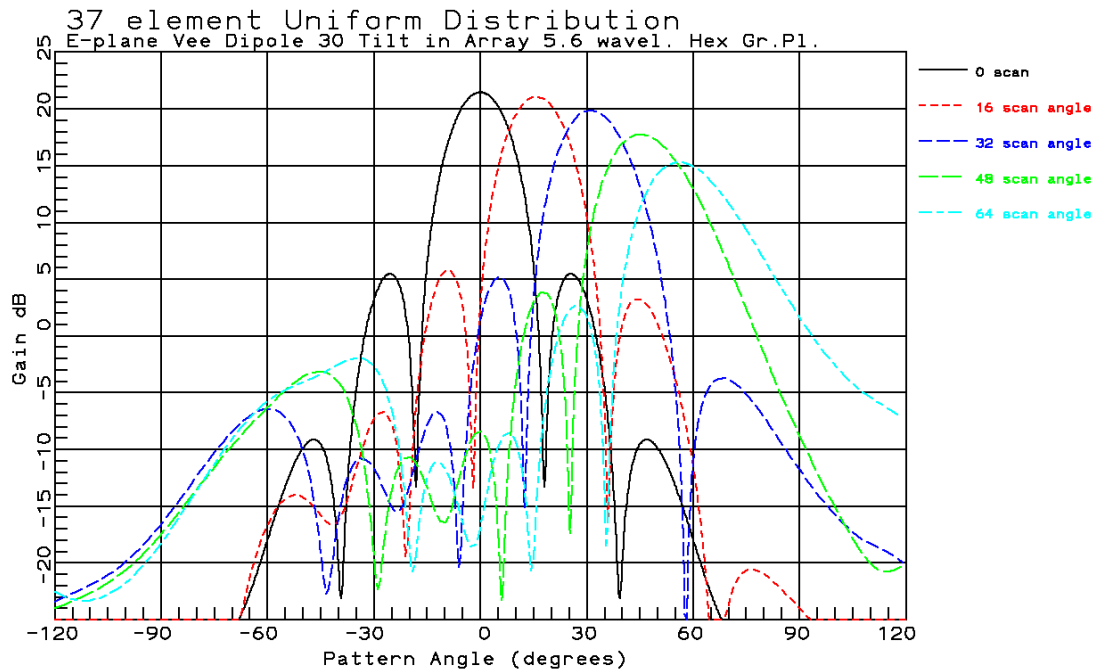


**Figure 12-5.1.37** *E*-Plane 37-element Uniform Distribution V-dipole hexagonal array spaced  $0.6\lambda$  mounted on  $5.6\lambda$  ground plane

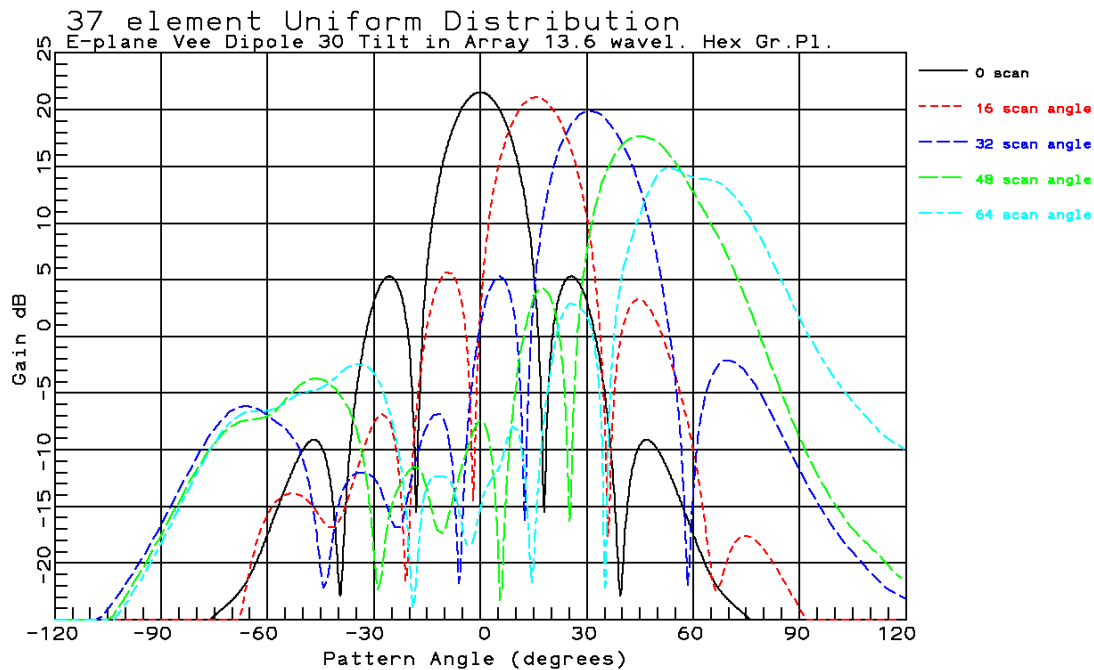


**Figure 12-5.1.38** *E*-Plane 37-element Uniform Distribution V-dipole hexagonal array spaced  $0.6\lambda$  mounted on  $13.6\lambda$  ground plane

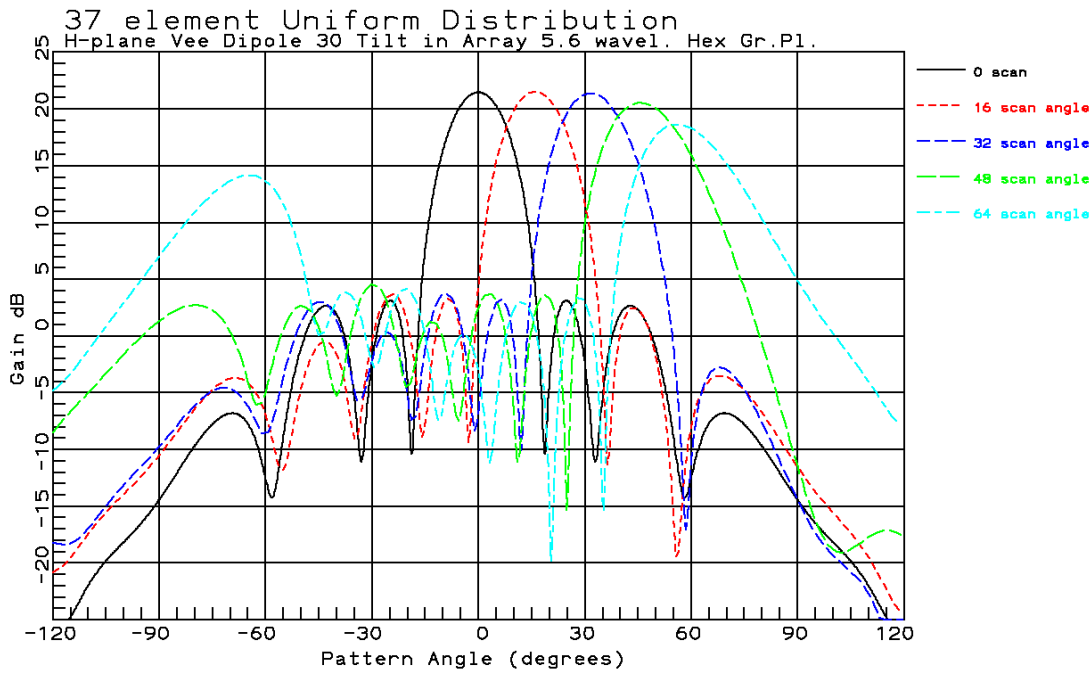


**Figure 12-5.1.39** H-Plane 37-element Uniform Distribution V-dipole hexagonal array spaced  $0.6\lambda$  mounted on  $5.6\lambda$  ground plane

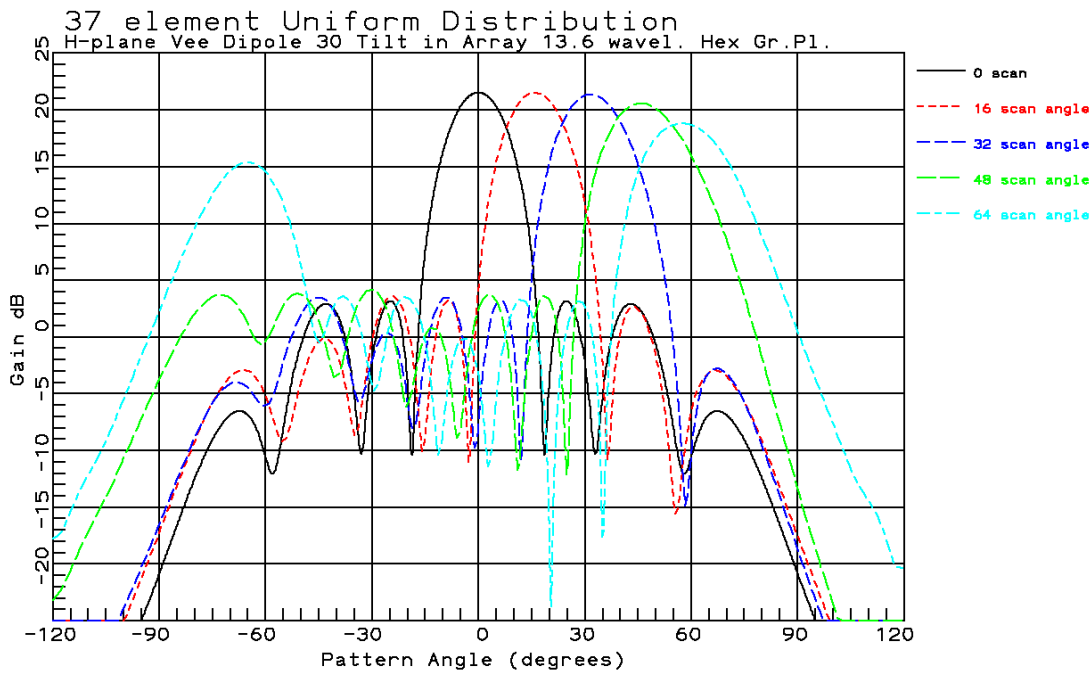


**Figure 12-5.1.40** H-Plane 37 element Uniform Distribution V-dipole hexagonal array spaced  $0.6\lambda$  mounted on  $13.6\lambda$  ground plane

## Chapter 12 Phased Arrays

Figures 37 - 40 plot the responses of a uniform distribution 37-element hexagonal array with  $0.6\lambda$  element spacing on a hexagonal ground plane with the edge element either  $1\lambda$  or  $5\lambda$  from the edge of the ground plane. The variation between the scan element patterns of the 37 elements averages out to form a beam peak which scans with similar shape from  $0^\circ$  to  $64^\circ$ . The main beam and sidelobes are similar whether on the smaller or larger ground plane. The hexagonal array first sidelobe is  $-16$  dB in the  $E$ -plane and  $-19.4$  dB in the  $H$ -plane which averages to  $17.7$  dB similar to a uniform circular distribution with a  $17.6$  dB first sidelobe. The larger ground plane reduces the backlobe region compared to the smaller one. The ripple in the  $E$ -plane due to the finite ground plane has little effect on the array pattern.

The  $E$ -plane of the hexagonal array can be scanned to  $90^\circ$  without the appearance of a grating lobe. When the array is scanned to  $64^\circ$  in the  $H$ -plane, a grating lobe is forming. Figure 41 of the grating lobe diagram shows the location of the emerging grating lobe.

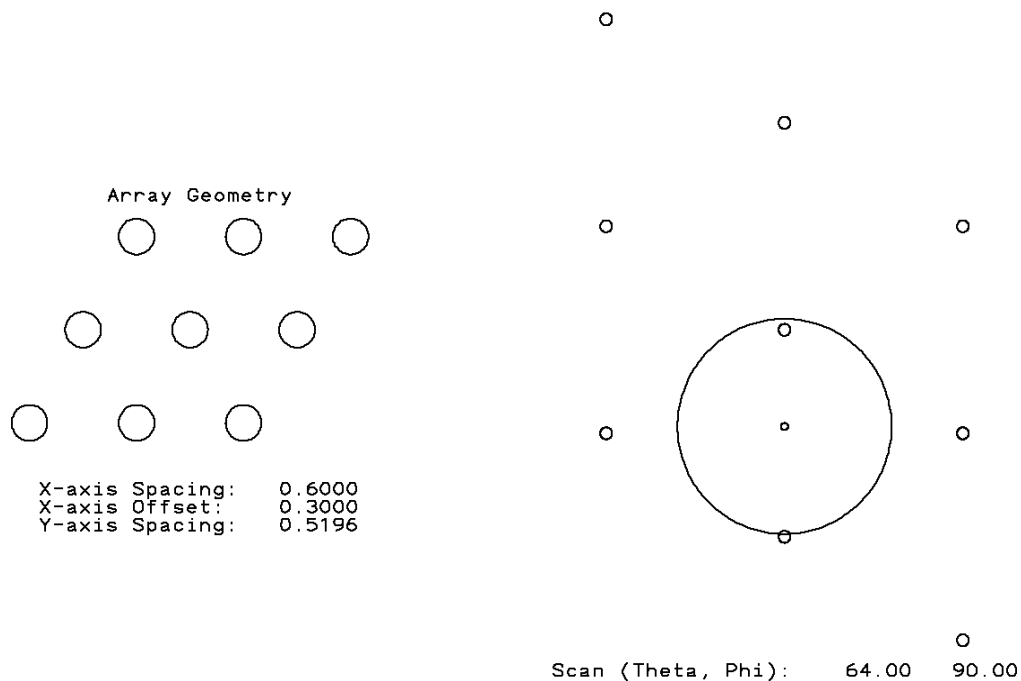


**Figure 12-5.1.41 Grating Lobe Diagram of  $0.6\lambda$  spaced Hexagonal Array in  $H$ -plane**

### Square Patch Array on Finite Polygon Ground Planes

Of course, patch arrays are mounted on finite ground planes which effects their patterns and makes direct measurement of scan element patterns troublesome. **SPAIMCP** computes patterns of arrays of square patches on polygon shaped ground planes. Similar programs: **CPAIMCP** and **RPAIMCP** perform calculations on circular or rectangular patches, respectively.

Close spacing between the patch and ground plane require fine PO segments to block magnetic currents from radiating to the backlobe. The plots below illustrate that the spacing has

## Chapter 12 Phased Arrays

insignificant effect on the upper hemisphere ripple but greater effect on the back hemisphere.

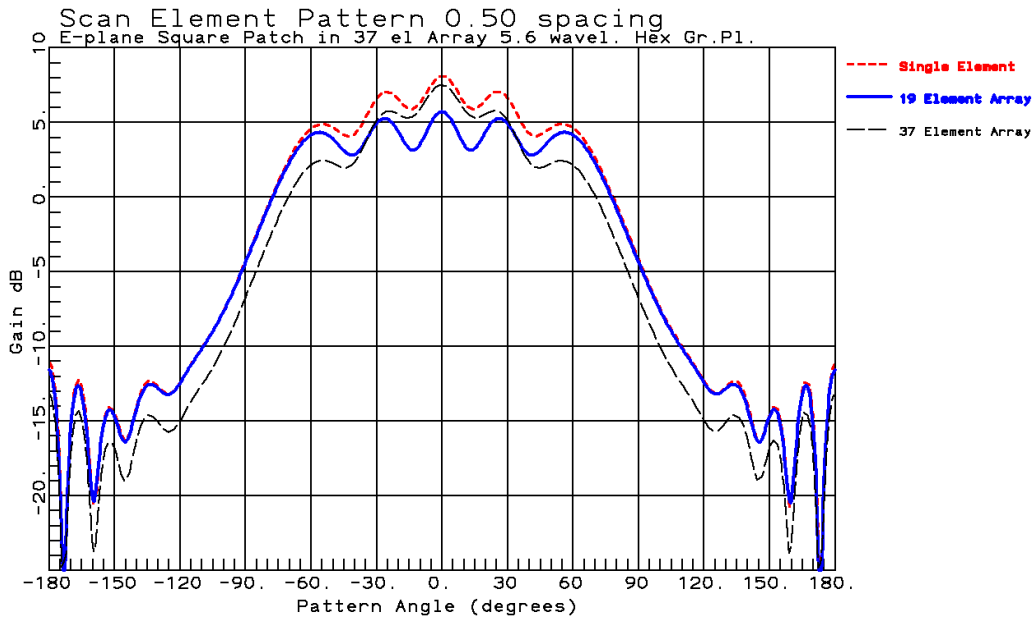


**Figure 12-5.1.42 Scan Element Pattern of Center Element of 19- and 37-element  $0.6\lambda$  spaced Hexagonal Array of Square Patches spaced  $0.04\lambda$  above  $5.6\lambda$  Ground Plane**

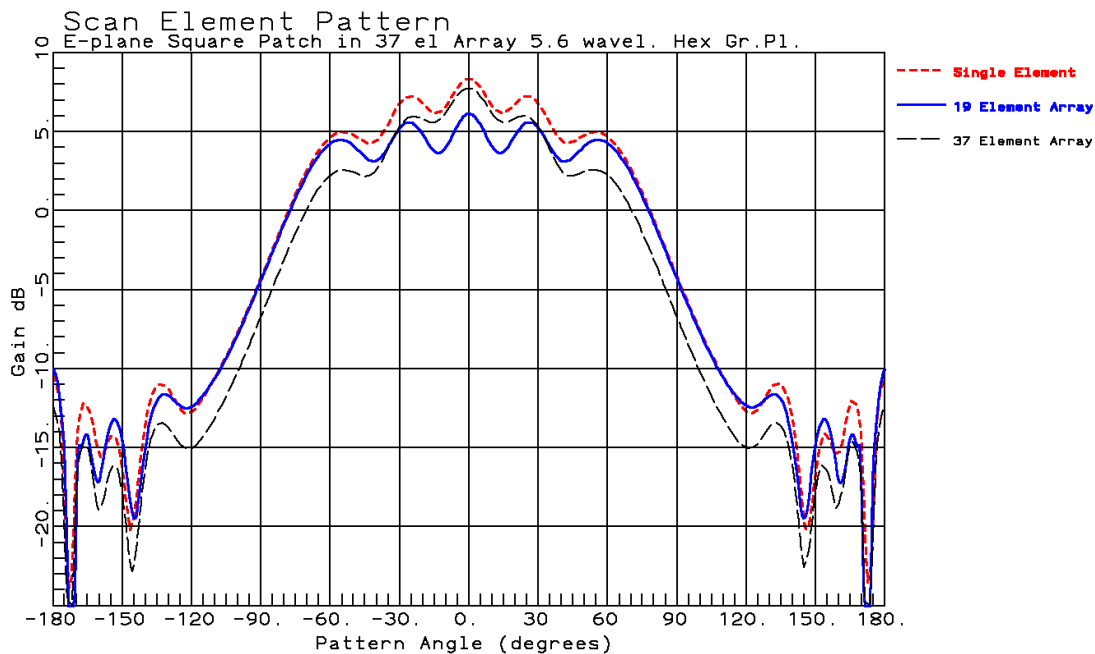


**Figure 12-5.1.43 Scan Element Pattern of Center Element of 19- and 37-element  $0.6\lambda$  spaced Hexagonal Array of Square Patches spaced  $0.02\lambda$  above  $5.6\lambda$  Ground Plane**

The  $5.6\lambda$  width ground plane has 6450 PO patches in both Figure 42 and 43 with similar results.

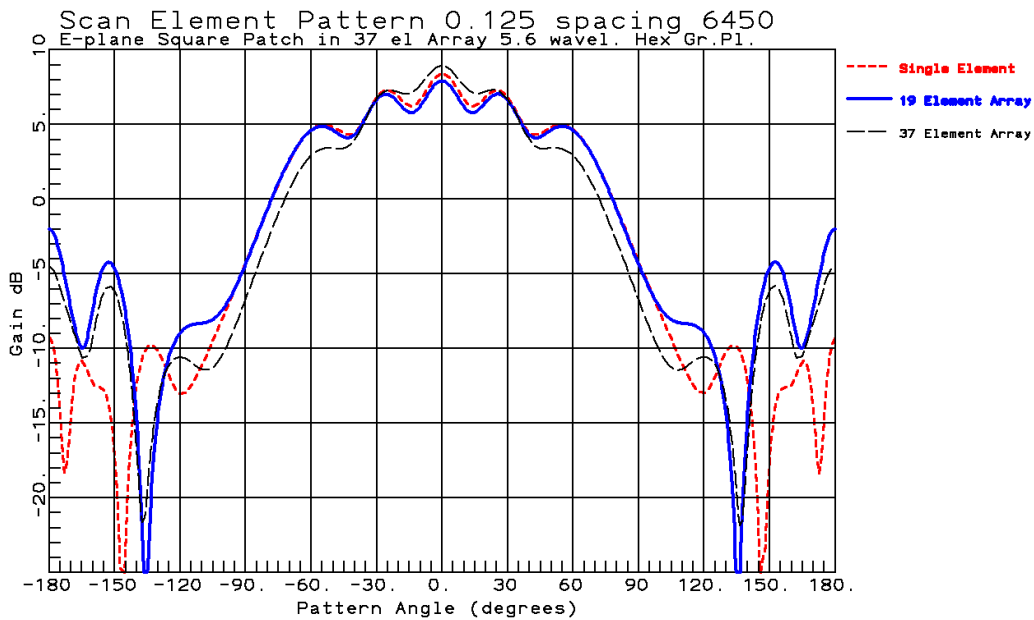


**Figure 12-5.144** Scan Element Pattern of Center Element of 19- and 37-element  $0.6\lambda$  spaced Hexangular Array of Square Patches spaced  $0.01\lambda$  above  $5.6\lambda$  Ground Plane

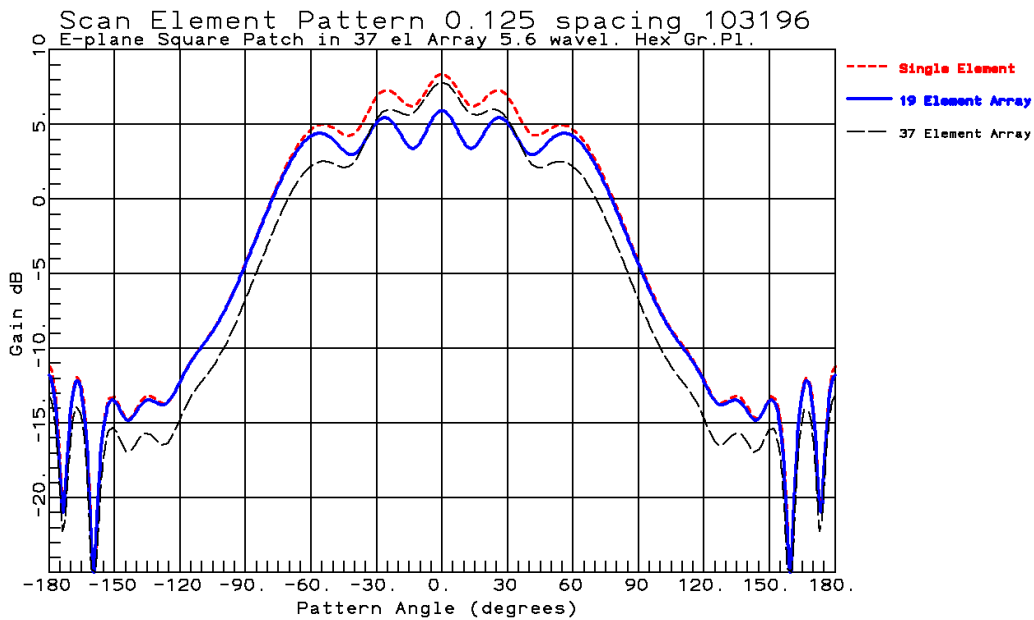


**Figure 12-5.145** Scan Element Pattern of Center Element of 19- and 37-element  $0.6\lambda$  spaced Hexangular Array of Square Patches spaced  $0.01\lambda$  above  $5.6\lambda$  Ground Plane

When the spacing has been reduced to  $0.01\lambda$  the number of PO patches has to be increased to 103,196 to achieve the same results as for the thicker spacing. Increasing PO ground plane patches increases runtime significantly. Ground plane spacing does not need to match substrate thickness.

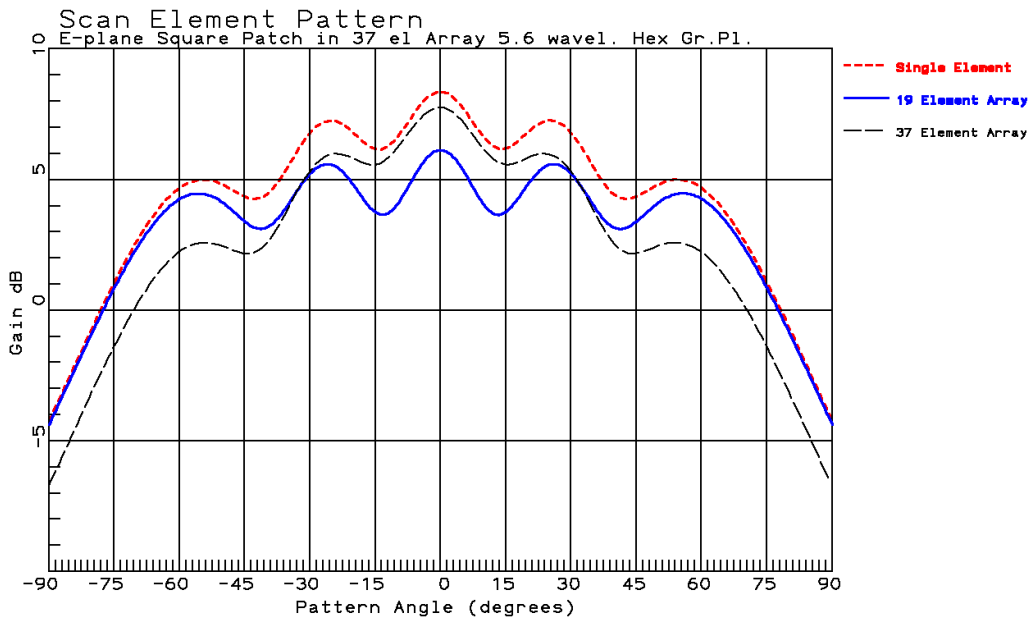


**Figure 12-5.1.46 E-plane Scan Element Pattern of Center Element of 19- and 37-element  $0.6\lambda$  spaced Hexagonal Array of Square Patches above  $5.6\lambda$  Ground Plane**

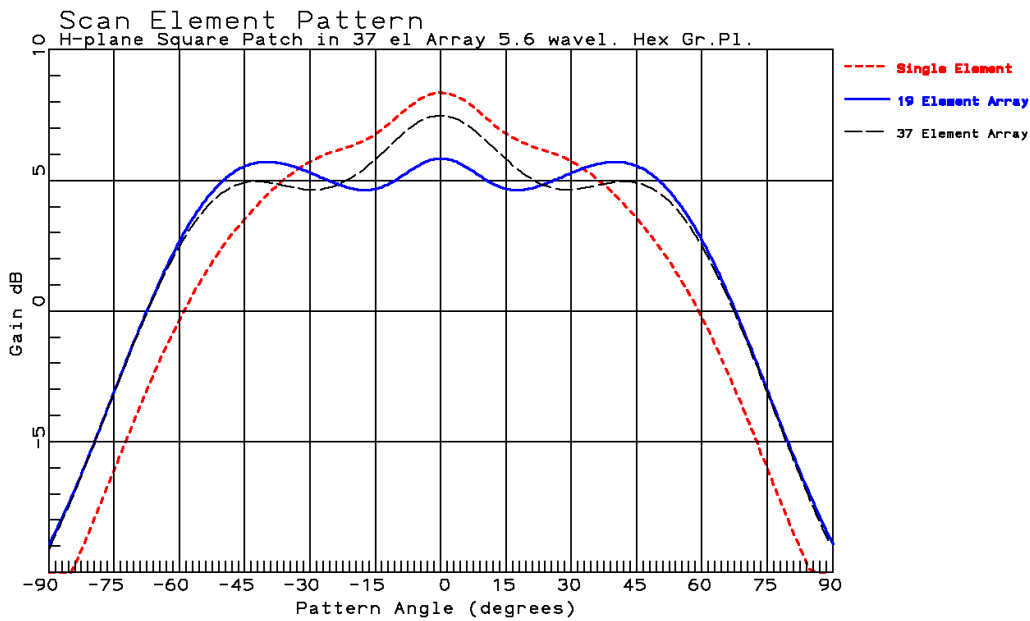


**Figure 12-5.1.47 H-plane Scan Element Pattern of Center Element of 19- and 37-element  $0.6\lambda$  spaced Hexagonal Array of Square Patches above  $5.6\lambda$  Ground Plane**

Figures 47 and 47 are similar to Figures 17 and 18 of the square patch on an infinite ground plane except the finite ground plane adds pattern ripple

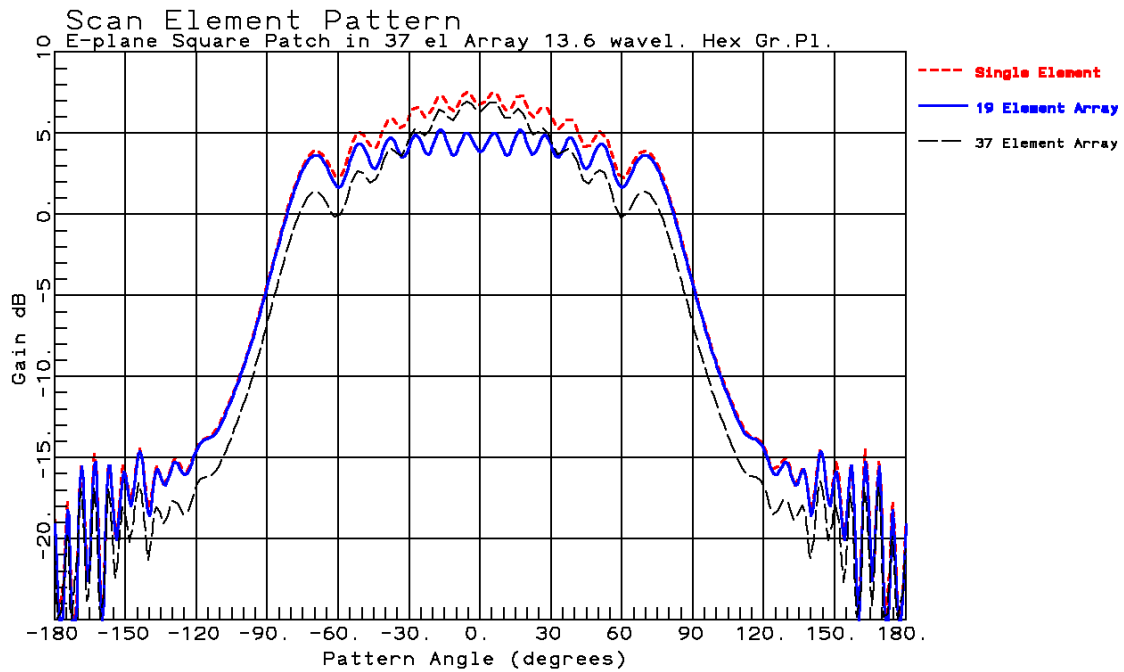


**Figure 12-5.148** *E*-plane Scan Element Pattern of Center Element of 19- and 37-element  $0.6\lambda$  spaced Hexagonal Array of Square Patches above  $13.6\lambda$  Ground Plane

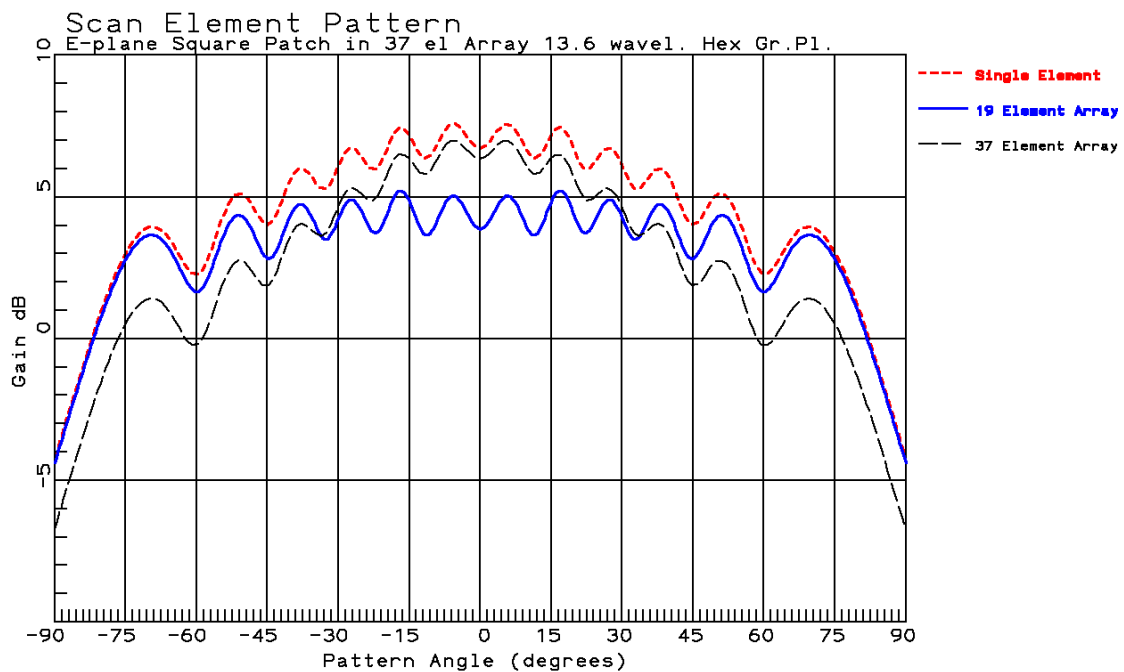


**Figure 12-5.149** *E*-plane Scan Element Pattern of Center Element of 19- and 37-element  $0.6\lambda$  spaced Hexagonal Array of Square Patches above  $13.6\lambda$  Ground Plane

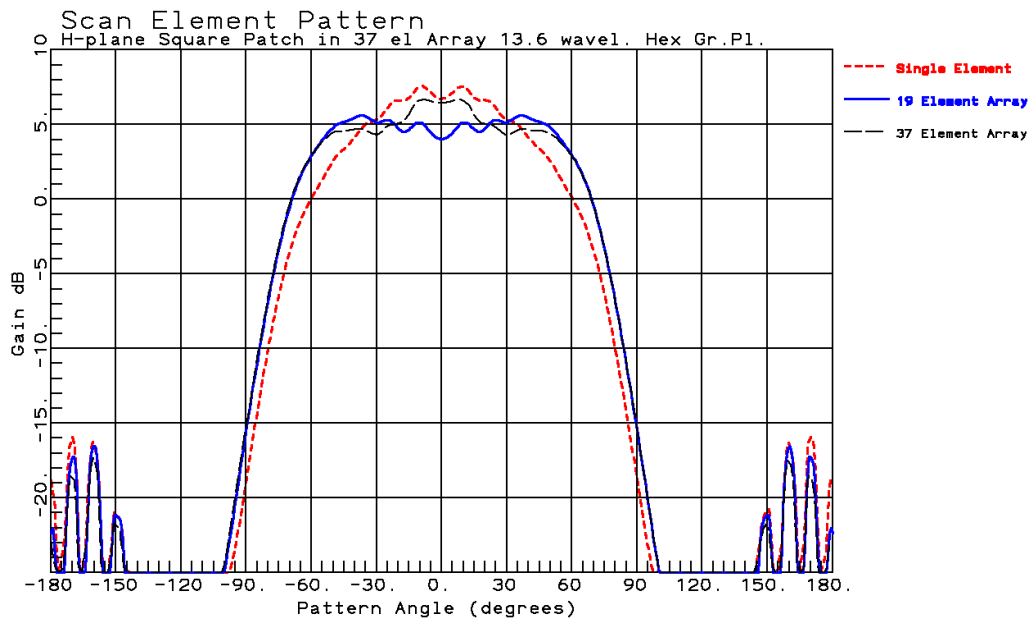


**Figure 12-5.150 H-plane Scan Element Pattern of Center Element of 19- and 37-element  $0.6\lambda$  spaced Hexagonal Array of Square Patches above  $13.6\lambda$  Ground Plane**

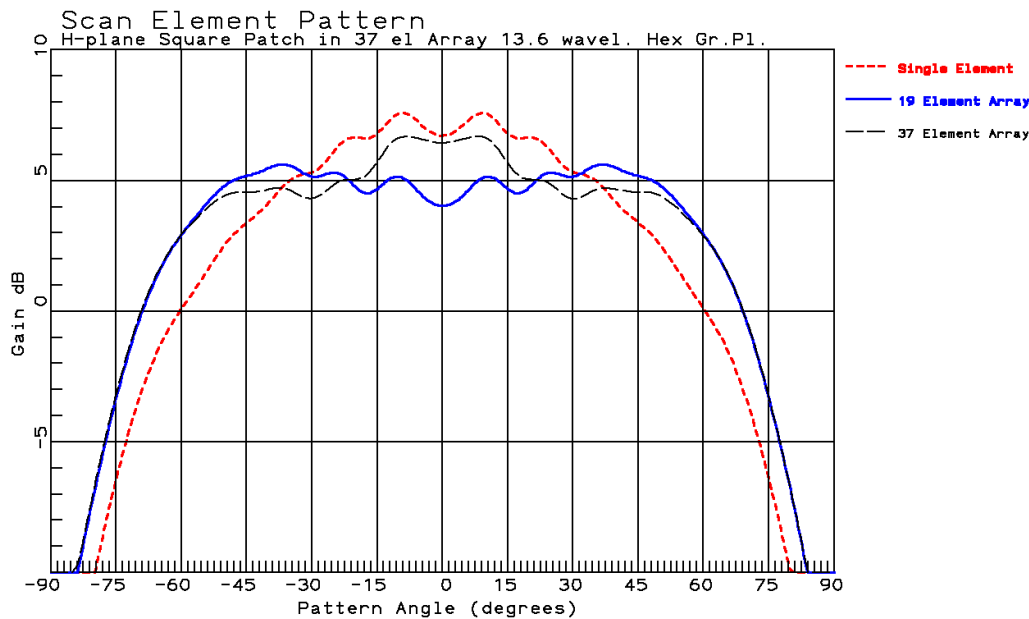


**Figure 12-5.151 H-plane Scan Element Pattern of Center Element of 19- and 37-element  $0.6\lambda$  spaced Hexagonal Array of Square Patches above  $13.6\lambda$  Ground Plane**

A uniformly fed 37-element hexagonal array of square patches were placed on  $5.6\lambda$  and  $13.6\lambda$  ground planes and scanned like the V-dipole examples above.

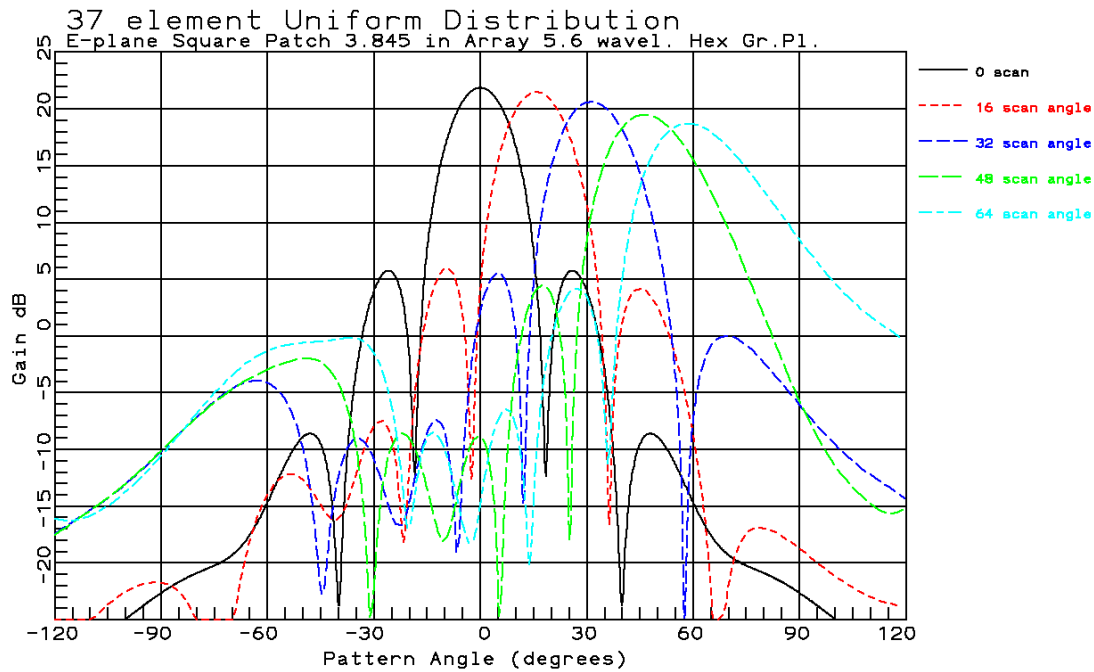


**Figure 12-5.1.52 E-Plane 37-element Uniform Distribution Square Patch hexagonal array spaced  $0.6\lambda$  mounted on  $5.6\lambda$  ground plane**

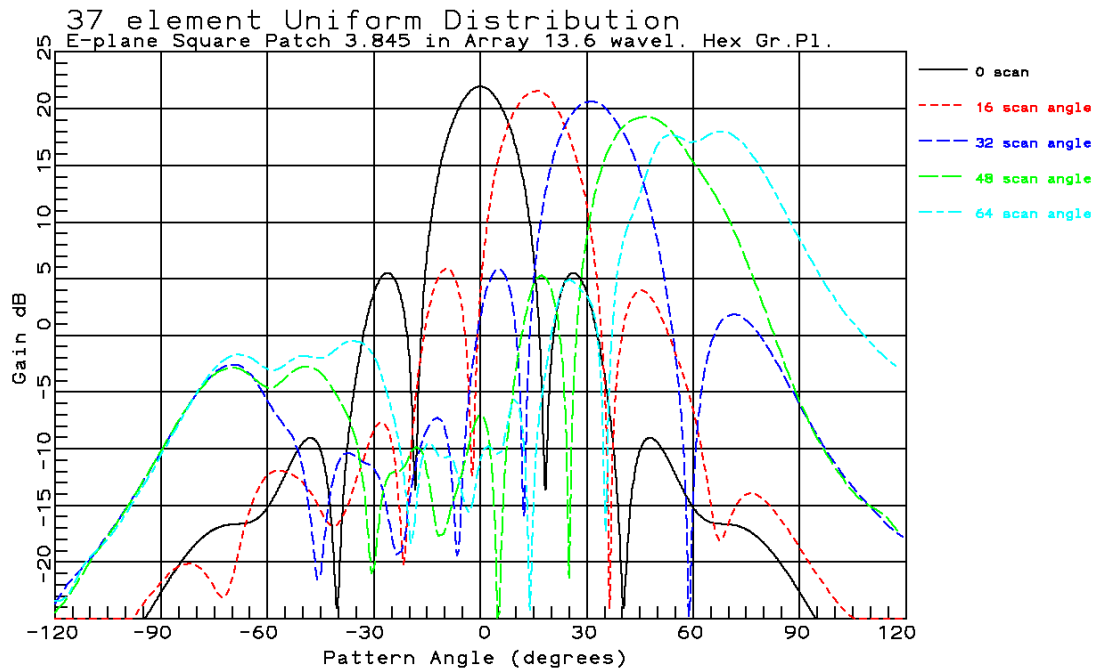


**Figure 12-5.1.53 E-Plane 37-element Uniform Distribution Square Patch hexagonal array spaced  $0.6\lambda$  mounted on  $13.6\lambda$  ground plane**

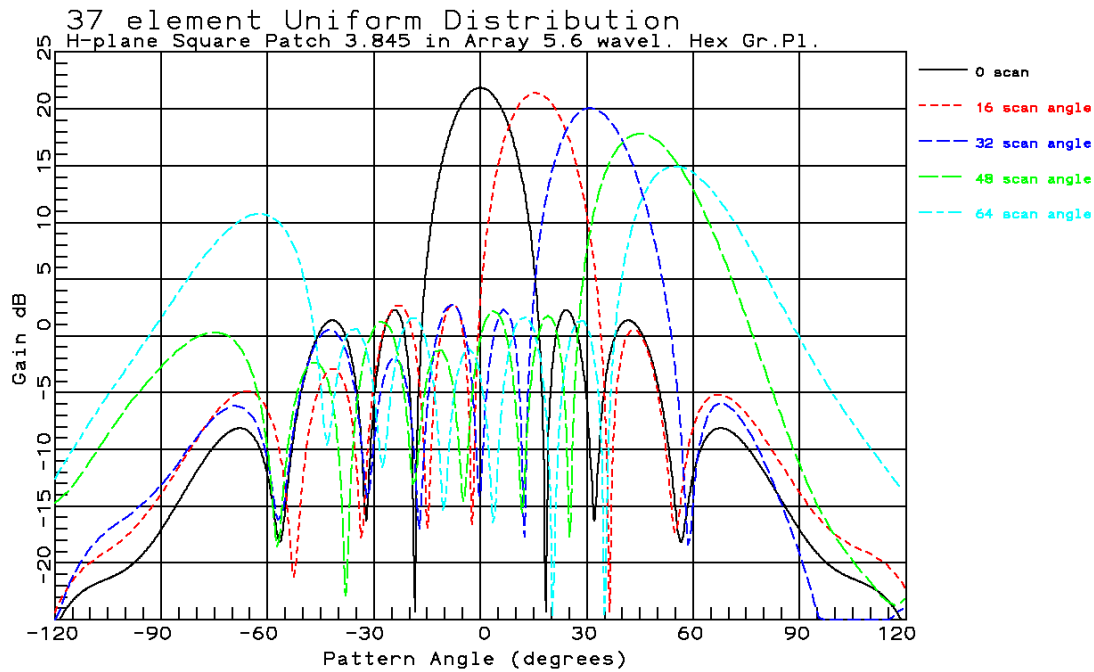


**Figure 12-5.154 H-Plane 37-element Uniform Distribution Square Patch hexagonal array spaced  $0.6\lambda$  mounted on  $5.6\lambda$  ground plane**

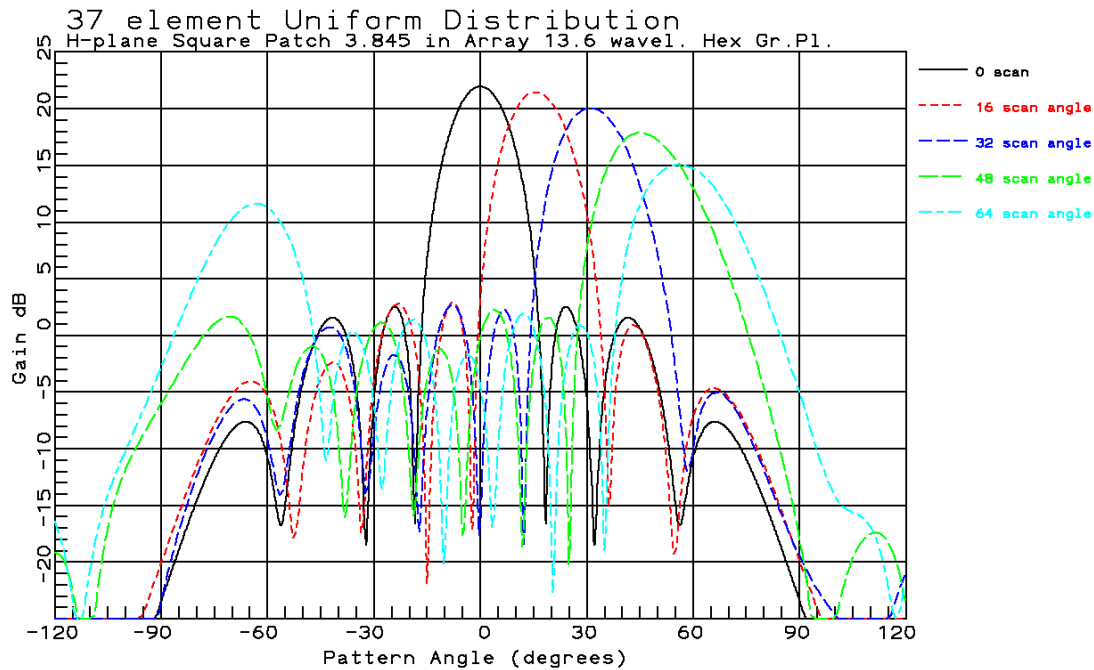


**Figure 12-5.155 H-Plane 37-element Uniform Distribution Square Patch hexagonal array spaced  $0.6\lambda$  mounted on  $13.6\lambda$  ground plane**